

R.C.M.N.S. Interim Colloquium



MARCH 2011 - SCONTRONE (L'AQUILA), ITALY

Field Guide to the Post-Conference Excursions (Scontrone, Palena and Montagna della Majella)

4 – 5 March 2011

Edited by

Giorgio CARNEVALE*, Etta PATACCA** & Paolo SCANDONE**

**Dipartimento di Scienze della Terra, Università degli Studi di Torino*

***Dipartimento di Scienze della Terra, Università di Pisa*

Itinerary of the excursions

Friday 4th March 2011

Departure from Castel di Sangro at 8.30 am.

Itinerary entirely on foot, starting from Scontrone at 9.00 am.

The excursion is aimed at illustrating some sections in the Scontrone Member of the *Lithothamnium* Limestone Formation, defining the stratigraphic position of the bonebeds and discussing the depositional environments/subenvironments of the Miocene deposits in the area. The location of the stops is indicated in the enclosed geological map.

Stop 1 Sangro Gorge (9.30.00-11.00 am)

Stop 2 Fossil Site (12.00-1.00 pm)

Lunch (1.00 -2.00 pm)

Stop 3 Scontrone South (3.00-4.00 pm)

Stop 4 Scontrone Cemetery (5.00-6.00 pm)

Return to Castel di Sangro at 6.30 pm.

Saturday 5th March 2011

Departure from Castel di Sangro at 8.30 am.

Itinerary by bus (about 300 kilometres) with short journeys by walking.

The excursion is aimed at showing the whole Bolognano Group and the overlying Tripoli Formation equivalent plus Gessoso-Solfifera Formation. In Southern Majella the Bolognano Group is characterized by the occurrence of disconformity surfaces with important hiatuses. In Northern Majella the amplitude of the gaps gradually decreases until the stratigraphic sequence become complete. In this area biostratigraphic data allow the attribution of the base and top of the *Lithothamnium* Limestone to the Tortonian and the early Messinian, respectively.

Travel by bus to Palena (30 Km)

Capo di Fiume Stop 1 Capo di Fiume section (9.30-10.30 am)

Majella Stop 1 Palena Cemetery section (10.45-11.15 am)

Majella Stop 2 Vallone di Taranta section (11.30 am-12.30)

Lunch (12.30-1.30 p.m.)

Travel by bus to the northern Majella region (110 Km)

Majella Stop 3 Messinian evaporites near San Valentino (3.00-4.00 pm)

Majella Stop 4 Roccamorice section (4.30-5.30 pm).

Return to Palena (110 Km)

Visit to the Alto-Aventino Geopaleontological Museum (7.00-8.00 pm).

Excursion
to Majella
5 March 2011



The post-Conference excursions will give the participants the opportunity to visit one of the most interesting regions of the Central-Southern Apennines (Fig. 1), where geology is quite complex but exposures are superb and subsurface features well known. A geological lineament running from the eastern foot of Majella to Alfedena (the latter is located just south of Scontrone), which corresponds to the emergence of the lateral ramp of a stack of rootless nappes transported over the Apulia foreland (Molise and Sannio Nappes), divides the region into two areas characterized by different structural architectures. In the western area the mountain chain consists of an imbricate fan of carbonate thrust sheets transported piggy-back towards the Adriatic Sea. These thrust sheets, grouped in major tectonic units that may reach a thickness of 5-6 kilometres, are composed of Mesozoic-Tertiary platform-derived and basin-derived carbonate sequences capped by siliciclastic flysch deposits (see Figs. 1, 2 and 3). The flysch deposits, Tortonian in the most internal (western) units, Messinian in the intermediate units and Pliocene in the most external ones, indicate the flexure-hinge retreat of the lower plate and the progressive forward migration of the thrust belt-foredeep-foreland system. In the eastern area, a pile of rootless nappes composed of Mesozoic-Tertiary basinal deposits up to 7-8 kilometres thick (Sannio and Molise nappes, the latter represented by the Frosolone, Agnone, Tufillo-Serra Palazzo and Daunia units) overlies a buried duplex system composed of Mesozoic-Tertiary platform carbonates with a very long thrust flat.

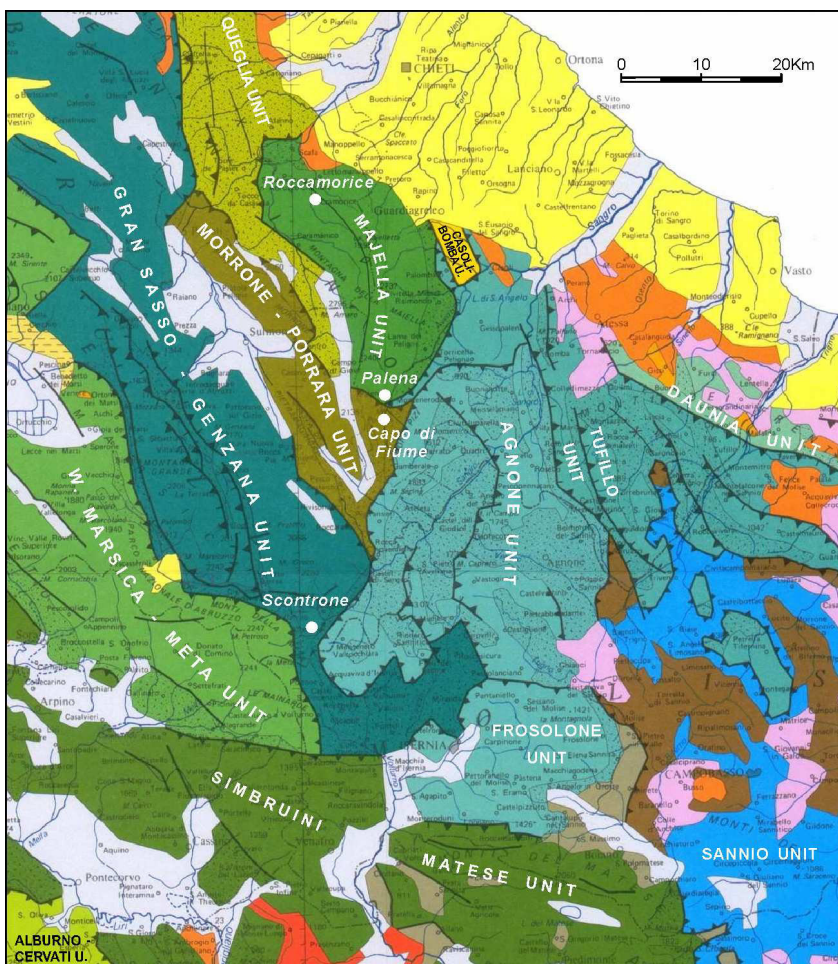


Figure 1. Simplified geological-structural map of the Abruzzi-Molise region. In the different tectonic units dots indicate siliciclastic flysch deposits. Brown, pink and orange colours refer to early Messinian, late Messinian and Pliocene thrust top deposits respectively, while yellow indicates post-orogenic Pleistocene deposits. Red refers to small outcrops of volcanites. Modified after Patacca & Scandone (2007).

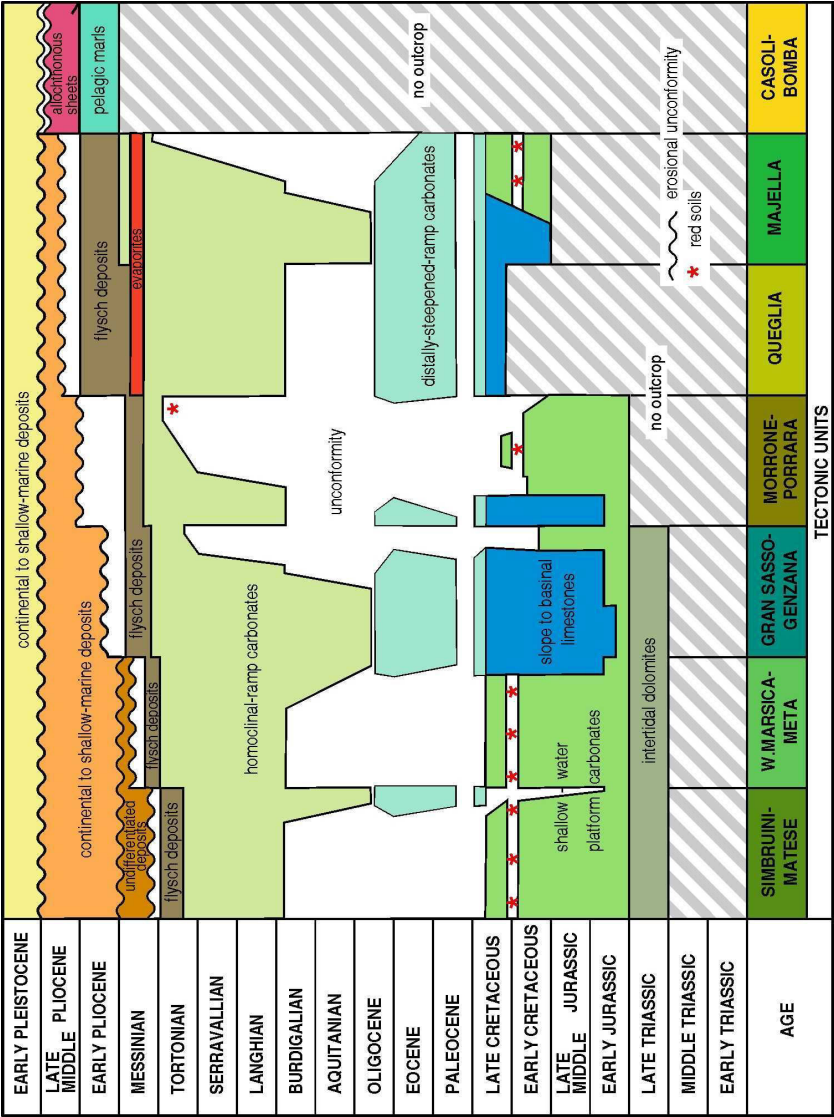


Figure 2. Stratigraphic sequences characterizing the tectonic units exposed in the western area. Modified after Patacca & Scandone (2007).

Before tectonic shortening, the buried carbonate duplex system was part of the Apulia Platform. The Majella and Morrone-Porrara units, which were incorporated in the mountain chain in the latest Messinian and in the early Pliocene, have also derived from this paleogeographic domain. Presently the Apulia Platform is a segment of the foreland of the peri-Adriatic fold-and-thrust belts. Before mountain building the Apulia Platform and the surrounding depositional domains constituted a complex system of platforms and basins the whose bulk originated in the middle Liassic consequently to the extensional tectonic processes that caused the dissection of an original upper Triassic-lower Liassic shallow epeiric area. The Lagonegro-Molise Basin is an exception in this framework since it formed around the end of the middle Triassic as a deep seaway linked, like the other Pindos-type basins of the Mediterranean region, towards the east with the pre-Jurassic Tethys Ocean. Around the end of the Cretaceous, platform edges turned into carbonate ramps characterized by overall prograding stacking pattern. Figure 4 shows a palinspastic restoration of the Apulia Platform and surrounding areas referred to the late Jurassic, around 150 Ma, a moment in which the paleogeographic characters of the different depositional domains were very well defined. In this reconstruction Apulia and the other segments of the Adriatic foreland have been rotated and translated more than 1500 kilometres SW of their present-day position according to the path of stable Africa with respect to Europe. The adjacent areas which during the Neogene were incorporated in the Apennine mountain chain have been relocated using classical criteria of retrodeformation and structural balancing. Figures 5 and 6 provide two images of the same area at Tertiary times in two very well documented moments. The first image refers to 29 Ma, when the “Mid-Oligocene” sea-level drop determined in the platform domains maximum subaerial exposure. The second one refers to 18 Ma (Burdigalian) when an important

transgressive event determined marine flooding over the greatest part of the platform areas.

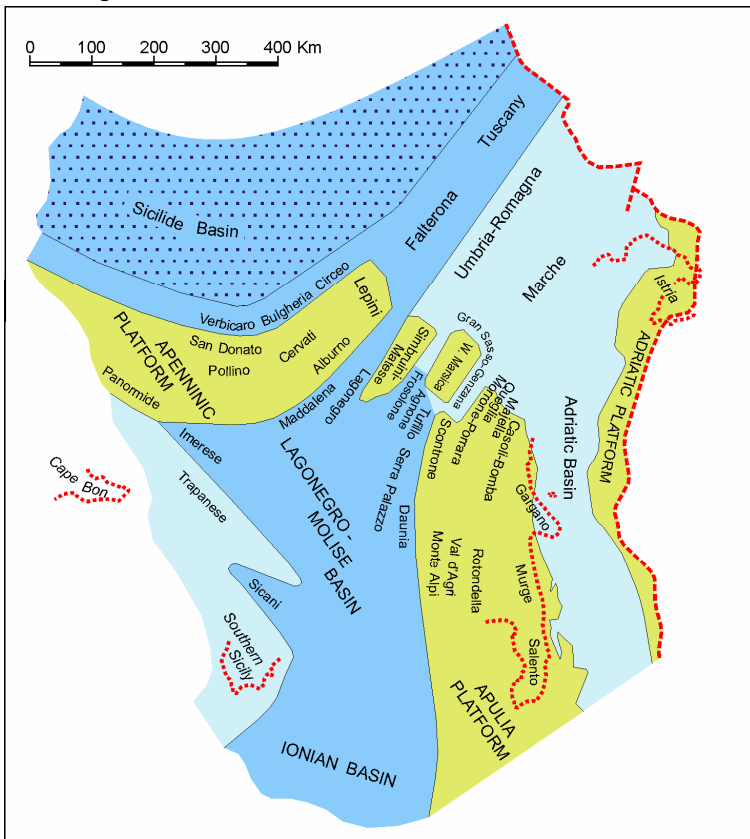


Figure 4. Palinspastic restoration of the Apulia Platform and surrounding platform-and-basin system in late Jurassic times (about 150 Ma). Green areas are Bahamian-type carbonate platforms separated by more or less deep basins (dark blue and light blue, respectively). The Sicilide and Lagonegro basins are supposed to have been floored, at least in part, by oceanic crust.

Note that in these palinspastic reconstructions the Apulia Platform was located about 290 kilometres SE of its present-day position in

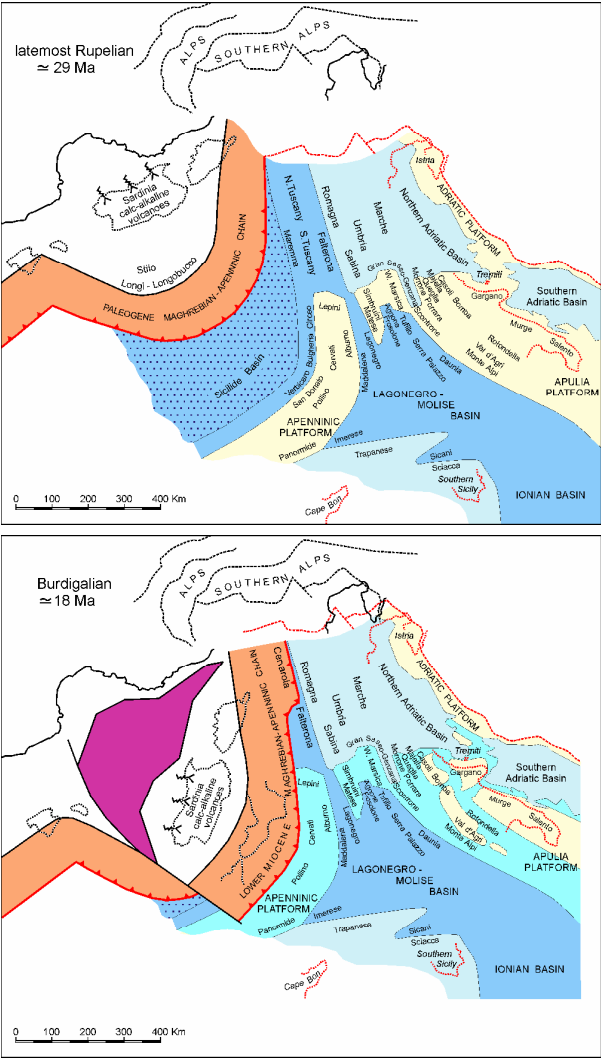


figure 5 and around 130 kilometres in figure 6.

Figure 5 and 6. Images of the Apulia and adjacent platform-and-basin system in a moment of maximum sea-level drop (Rupelian, 29 Ma) and in a moment of maximum transgression (Burdigalian, 18 Ma). After the Burdigalian the compression front in the Central-Southern Apennines moved around 400 kilometres towards the east reaching in the early Pleistocene the position indicated in figure 7.

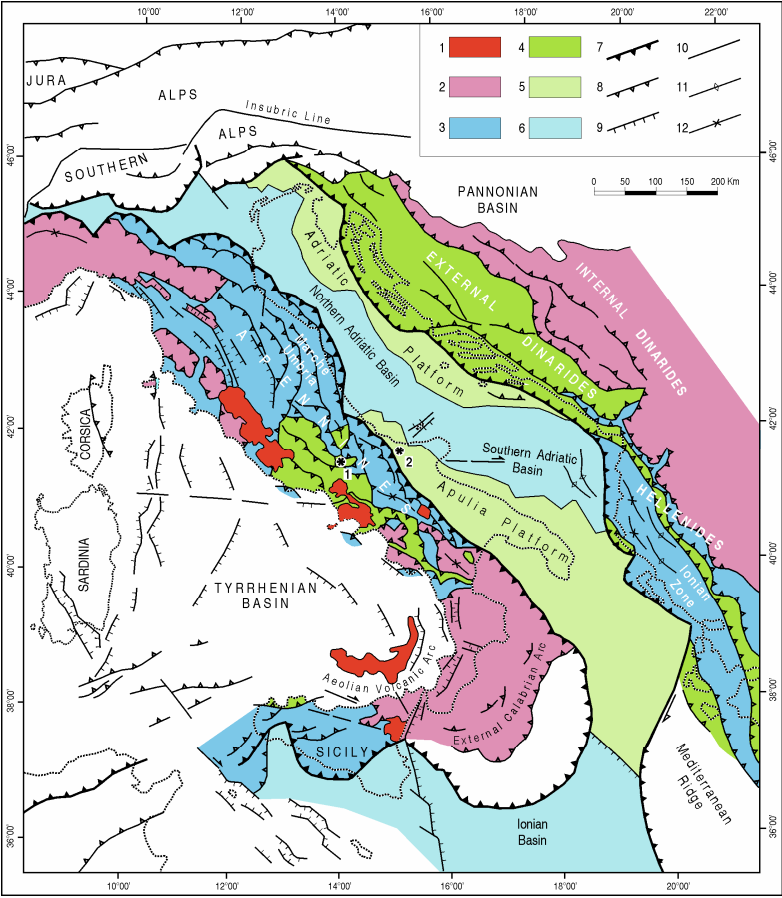


Figure 7. Tectonic lineaments of the peri-Adriatic region with the distribution of the platforms and basins in the foreland areas and the distinction between platform-derived and basin-derived tectonic units in the Apennines and Dinarides. Asterisks indicate the Scontrone (1) and Gargano (2) fossil sites. After Patacca et al. (2008).

1, Major subaerial Quaternary volcanoes. 2, Undifferentiated internal units of the Apennines, Calabrian Arc and Dinarides-Hellenides. 3, External units of the Apennines, Sicilian Maghrebides and Dinarides-Hellenides chiefly represented by Mesozoic-Tertiary basinal and pelagic carbonate sequences. 4, External units of the Apennines-Sicilian Maghrebides and Dinarides-Hellenides mostly represented by Mesozoic-Tertiary shallow-water carbonate sequences. 5, Foreland areas characterized by Mesozoic-Tertiary basinal and pelagic carbonate sequences. 6, Foreland areas characterized by thick Mesozoic-Tertiary shallow-water carbonate sequences. 7, Front of the Sicilian Maghrebides, Apennines, Alps, Southern Alps and Dinarides-Hellenides. 8, Major thrusts. 9, Normal faults. 10, High-angle faults, mostly strike-slip faults. 11, Anticline axis. 12, Syncline axis.

References

- PATACCA E. & SCANDONE P. (2007) – Geology of the Southern Apennines. In MAZZOTTI A., PATACCA E. & SCANDONE P. (Eds), Results of the CROP Project, Sub-project CROP-04 Southern Apennines (Italy). *Bollettino della Società Geologica Italiana (Italian Journal of Geosciences)*, Special Issue 7: 75-119.
- PATACCA E., SCANDONE P. & MAZZA P. (2008) – Oligocene migration path for Apulia macromammals: the Central-Adriatic bridge. *Bollettino della Società Geologica Italiana (Italian Journal of Geosciences)*, 127: 337-355.

Excursion 1: Scontrone, 4th March 2011.

GEOLOGICAL FRAMEWORK OF THE SCONTRONE AREA

Etta PATACCA & Paolo SCANDONE

Dipartimento di Scienze della Terra, Università di Pisa

In the Scontrone area an interesting stratigraphic sequence composed of Mesozoic-Tertiary carbonates crops out with very good exposures. This sequence is referable to the Gran Sasso-Genzana Unit, a cover nappe that extends from Northern Abruzzi to Alto Molise forming the bonebed of the Central Apennines, with mountains exceeding 2000 metres in elevation and with Corno Grande, the highest peak of Gran Sasso, reaching 2912 metres above sea level. The carbonate deposits are conformably overlain by siliciclastic flysch deposits of Messinian age. In the Scontrone area, the flysch deposits (Castelnuovo al Volturno Wildflysch, Patacca et al., 1990) contain huge olistostromes and olistoliths of Cretaceous-Miocene basinal deposits, which have derived from the Molise Nappe during their forward displacement towards the Apulia foreland.

In a palinspastic restoration referred to late Jurassic-early Cretaceous times, the Scontrone area lies in correspondence to the southward termination of the Gran Sasso-Genzana Basin against the

north-western margin of the Apulia Platform (fig. 1). This paleogeographic reconstruction is well documented by the facies of the Jurassic-Cretaceous carbonates of Scontrone which are indicative of platform margin, slope and proximal basin. Following the strike of the tectonic structures within the Gran Sasso-Genzana nappe, typical basinal deposits are exposed a few kilometres north of Scontrone, e.g. at Monte Greco and Monte Genzana, whilst coeval shallow-platform carbonates are exposed a few kilometres south of Scontrone at Monte La Rocca and Monte San Michele (High Volturno Valley).

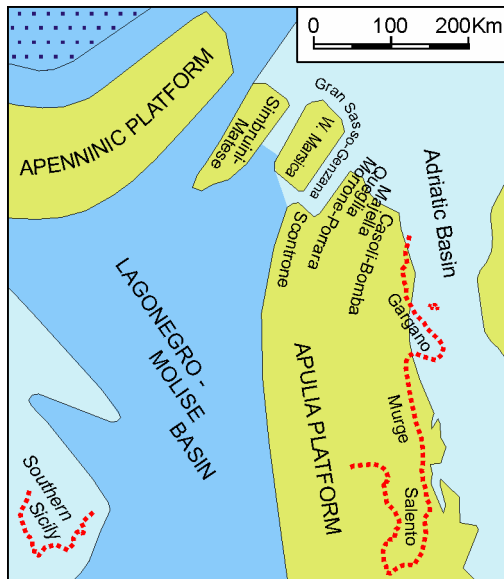


Figure 1. Palinspastic restoration of the platform-and-basin system of the Central-Southern Apennines during late Jurassic times (about 150 Ma). The picture shows the southern termination of the Gran Sasso-Genzana Basin against the Apulia Platform in correspondence to the Scontrone paleogeographic domain.

North of Scontrone, the stratigraphic sequence is basically made up of upper Triassic-lower Liassic shallow-water carbonates followed by middle Liassic-Paleogene basinal deposits which are covered, in turn, by uppermost Oligocene-upper Miocene outer-ramp carbonates. South of Scontrone, on the contrary, the stratigraphic sequences are characterized by persisting shallow-water conditions through Mesozoic times, with Neocomian platform-margin limestones and adjacent platform-interior carbonates unconformably overlain by upper Miocene inner to outer-ramp carbonate deposits. In the Scontrone area an almost complete sequence with transitional characteristics is exposed in the Sangro Gorge between Scontrone and Barrea (see enclosed geological map in foldout 1). The sedimentary sequence is represented in this area by Neocomian-Barremian platform-edge carbonates and marginal-slope megabreccias (uppermost portion of the Terratta Formation and Coral-bearing Calcirudite, respectively) disconformably overlain by slope-apron bioclastic calcarenites and calcirudites (Rudist-bearing Calcarenite, upper Albian-Turonian) followed by Coniacian-Campanian hemipelagic limestones with frequent intercalations of calciturbidite beds and lime debrites. The Neocomian-Campanian platform-to-basin depositional system, featured as a retreating margin, evolved from the latest Maastrichtian into an overall prograding carbonate ramp punctuated by several unconformities with more or less prolonged temporal hiatuses. Outer-ramp bioclastic calcarenites of Maastrichtian age (Saccharoidal Limestone) are locally overlain by upper Paleocene fore-reef calcirudites (Coral-algal Limestone). The latter suggest proximity to a warm-water reefal slope belonging to a distally-steepened carbonate-ramp system. Upper Miocene cool-water shallow-marine carbonates (*Lithothamnium* Limestone) directly overlie the Cretaceous deposits, locally with an intervening discontinuous veneer of upper Paleocene coral breccias. The

Lithothamnium limestones grade upward into hemipelagic deposits (*Turborotalia multiloba* Marl). The deepening-up stratal architecture of the *Lithothamnium* Limestone-*T. multiloba* Marl indicates a gently subsiding homoclinal ramp. The onset of siliciclastic flysch deposits temporally constrains the incorporation of the Scontrone foreland domain in the Apennine foredeep basin in a well-defined moment of the Messinian after the first common occurrence of *Turborotalia multiloba* and before the beginning of the salinity crisis.

Figure 2 provides a stratigraphic scheme that describes the primary relationships between the lithostratigraphic units composing the

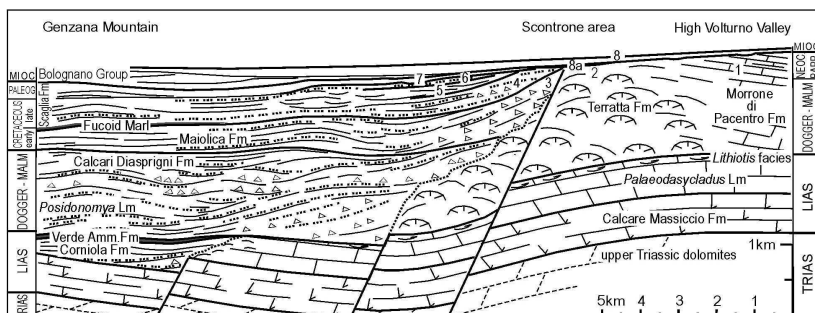


Figure 2. Stratigraphic architecture of the Mesozoic-Tertiary carbonates of the Gran Sasso-Genzana Unit between the Genzana Mountain and the High Volturno Valley (after Patacca et al. 2008 with slight modifications). The Arabic numerals 1-8a refer to the lithostratigraphic units (or portions of lithostratigraphic units) cropping out in the Scontrone area and, a few kilometres towards the south, in the High Volturno region: 1) Neocomian-Barremian platform-interior limestones (Morrone di Pacentro Fm p.p.); 2) Neocomian-Barremian platform-edge limestones (Terratta Fm p.p.); 3) Neocomian-Barremian marginal slope-breccias (Coral-bearing Calcirudite); 4) Upper Albian-Turonian slope-apron calcarenites (Rudist-bearing Calcarenite); 5) Coniacian-Campanian hemipelagic limestones and platform-derived lime resediments with fragments of rudists (Scaglia Fm); 6) Maastrichtian outer ramp biocalcarenes (Saccharoidal Limestone); 7)

Upper Paleocene breccias with clasts of reefal limestones (Coral-algal Limestone); 8) Tortonian-lowermost Messinian rhodalgial ramp carbonates (Lithothamnium Limestone); 8a) Tortonian peritidal carbonates (Scontrone Member of the Lithothamnium Limestone).

Gran Sasso-Genzana nappe in an area that extends from the Monte Genzana (north) to the High Volturno Valley (south).

The itinerary of the excursion is limited to Scontrone outskirts, but spectacular panoramic views, mainly from stop 1 and stop 3, will allow the participants to get a realistic idea of the geological characteristics of this interesting piece of Apennines.

References

- PATACCA E., SARTORI R. & SCANDONE P. (1990) – Tyrrhenian basin and Apenninic arcs: kinematic relations since Late Tortonian times. *Memorie della Società Geologica Italiana*, 45: 425-451.
- PATACCA E., SCANDONE P. & MAZZA P. (2008) – The Miocene land-vertebrate fossil site of Scontrone (Central Apennines, Italy). *Bollettino della Società Geologica Italiana (Italian Journal of Geosciences)*, 127: 51-7.

THE MIOCENE DEPOSITS OF SCONTRONE

Etta PATACCA* & Paolo SCANDONE* & Giorgio CARNEVALE**

*Dipartimento di Scienze della Terra. Università di Pisa

**Dipartimento di Scienze della Terra. Università degli Studi di Torino

The Scontrone vertebrate remains are contained in the transgressive basal portion of the *Lithothamnium* Limestone Formation (Scontrone Member of the *Lithothamnium* Limestone in Patacca et al., 2008) which overlies in unconformity different terms of the Cretaceous-Paleocene sequence with a temporal gap spanning between 45 and 80 Ma north-west of Scontrone and reaching at least 120 Ma south-east of the village (see geological map in foldout 1, columnar sections in foldout 2, and their geographic location in Fig.

1). A complete section of the Scontrone Member crops out in the



Figure 1. Panoramic view on Scontrone showing the location of the stratigraphic sections described in the text and illustrated as columnar sections in foldout 2.

Sangro Gorge on top of upper Paleocene calcirudites characterized by huge clasts of *Polysrta alba* and *Archeolithothamnium* boundstones (Coral-algal Limestone). The Thanetian age of these deposits is indicated by the presence of *Planomalina cretae*, *Miscellanea* sp., *Cuvillierina* sp., *Discocyclus* sp. and rare *Morozovella* sp. recovered in the matrix of the breccias. In the Scontrone North and Scontrone Fossil Site sections the Scontrone Member overlies in disconformity upper Albian-Turonian skeletal debrites and redeposited litho-bioclastic calcarenites rich in echinodermal plates, fragments of corals, well-rounded fragments of rudists (requienids) and oversized calcareous lithoclasts (Rudist-bearing Calcarenite; Fig. 2.1). These resediments have obviously derived from penecontemporaneous high-energy shoals connected with rudist banks. In the lower/middle part of the Rudist-bearing Calcarenite the dominant lithologies are represented by bioclastic packstones

with orbitolinids and fragments of caprinids. Sporadic intercalations of hemipelagic foraminiferal wackestones document the late Albian *Rotalipora ticinensis* Zone (*Hedbergella*, *Ticinella* and *Globigerinelloides* associated with *Rotalipora ticinensis*, *Ticinella roberti*, *Biticinella breggiensis* and *Planomalina buxtorfi*). The fossil content in the upper portion of the Rudist-bearing Calcarenites is mostly represented by fragmented radiolitids, *Pithonella*-like calcisphaerulids and echinodermal plates associated with sporadic planktonic foraminifers (*Praeglobotruncana gibba* and *Dicarinella imbricata*) attesting the Cenomanian-Turonian (*Whiteinella archeocretacea* and *Helvetotruncana helvetica* Zones). In the Scontrone Fossil Site area the first occurrence of *Marginotruncana pseudolinneiana* and *M. coronata* in the uppermost portion of the Rudist-bearing Calcarenites documents the middle/late Turonian. In the Scontrone South section the Scontrone Member lies above the Neocomian-Barremian platform-edge carbonates of the Terratta Formation represented by reefal boundstones with a rich and extremely diversified fossil assemblage

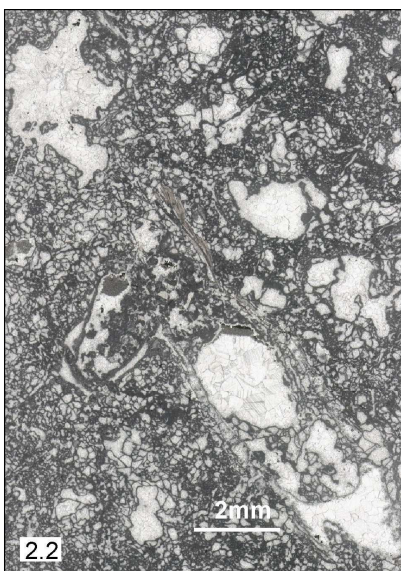
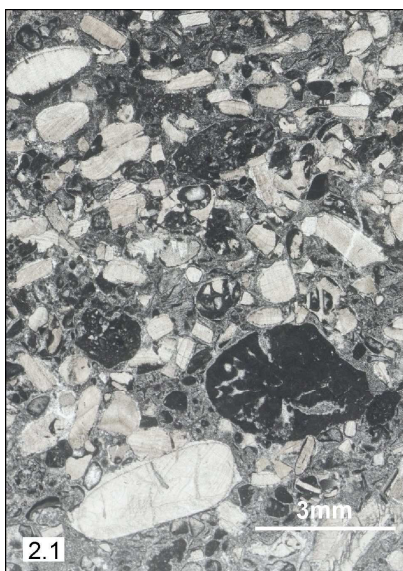


Figure 2.1. Scontrone Cemetery section. Litho-bioclastic packstone with very well-rounded fragments of rudists (requienids) and oversized

calcareous lithoclasts. In the lower-right side, intensively bored lithoclast. Upper Albian-Turonian Rudist-bearing Calcareenite. **2.2.** Scontrone South section. *Bacinella irregularis*/*Lithocodium aggregatum* boundstone. Neocomian-Barremian Terratta Formation. **2.3.** Scontrone North section. Lithobioclastic grainstone/packstone with numerous thick-shelled *Ammonia* and porcellanaceous benthic forams. Scontrone Member of the Lithothamnium Limestone, interval **a**. **2.4.** Sangro Gorge section. Bioclastic packstone with *Ammonia* and *Elphidium*. The bifurcating, thinning downward large tubular structure coated by a thick dense micrite is a rhizolith structure. Scontrone Member of the Lithothamnium Limestone, upper portion of the **a** interval.

including stromatoporoids, crinoidal plates, calcareous sponge, *Tubiphytes morronensis*, *Cayeuxia* and *Bacinella irregularis*/*Lithocodium aggregatum* (Fig. 2.2) locally associated with *Nautiloculina* spp., *Trocholina* spp. and *Protopenneroplis ultragranulata*.

The Scontrone Member of the *Lithothamnium* Limestone (Patacca et al., 2008) represents a fortuitous relic of paralic deposits escaped from the erosive ravinement usually accompanying the shallow-marine Tortonian transgression. In the outskirts of Scontrone these paralic deposits display rapid facies variations within a quite small area (see columnar sections in foldout 2). The complex lateral variations and stratal architecture, which made difficult correlations from one site to the other, required detailed stratigraphic and sedimentological analyses. In this guidebook the Scontrone Member has been divided into four intervals featuring two major parasequences. The lower parasequence, ranging in thickness from 8 metres in the Sangro Gorge section to 3 metres in the Scontrone Fossil Site and Scontrone South-West sections and characterised by an overall shallowing and thinning-up stratal architecture, has been referred to a storm-dominated coastal environment. The overlying thicker parasequence, which directly

onlaps the Neocomian platform margin in the Scontrone South area, is characterized as a whole by a shallowing and coarsening-up stratal architecture. The deposition of this parasequence took place in a wave-dominated barrier-lagoon coastal setting. The second parasequence of the Scontrone Member is truncated at the top by a ravinement surface developed at the base of the high-energy shallow-marine carbonates forming the lower portion of the Lithothamnium Limestone Formation in the bulk of the Central Apennines where the Scontrone Member is lacking.

The transgressive tract of the lower parasequence, representative of high-energy coastal bars (interval a in the columnar sections of foldout 2), consists of 2.5 metres of buff to off-white mottled calcarenites locally showing a faint large-scale and low-angle cross stratification. In thin section these calcarenites are represented by litho-bioclastic grainstone/packstones with abundant large-sized *Ammonia* and frequent *Elphidium crispum* together with relatively abundant porcellanaceous benthic foraminifers (Fig. 2.3). The *Ammonia*-and-*Elphidium* association indicates a nearshore environment with clean-hard substrate. The lithoclasts, all very well rounded and often bored, have derived from older well-lithified lithologies. In addition, the presence of abraded specimens of isolated late Cretaceous globotruncanids and of micritized Paleogene-early Miocene large foraminifers indicates strong subaerial erosion and severe physical reworking and winnowing of the eroded material. Near the top, the bio-lithoclastic calcarenites show vertically-elongated root traces with their micritic coating, as well as strong bioturbation (Fig. 2.4). A thin layer (20-25 centimetres) of pervasively rooted, yellow-to-pink very-fine-grained calcarenite (Fig. 3.1) lies on top of the shallow-water calcareous sand bars. This calcarenite is characterized by very well-rounded mostly biogenic carbonate grains set in a reddish FeO-stained dense micrite matrix of pedogenic origin. The calcarenite layer has been interpreted as a

supratidal wind-driven deposit marking the beginning of the

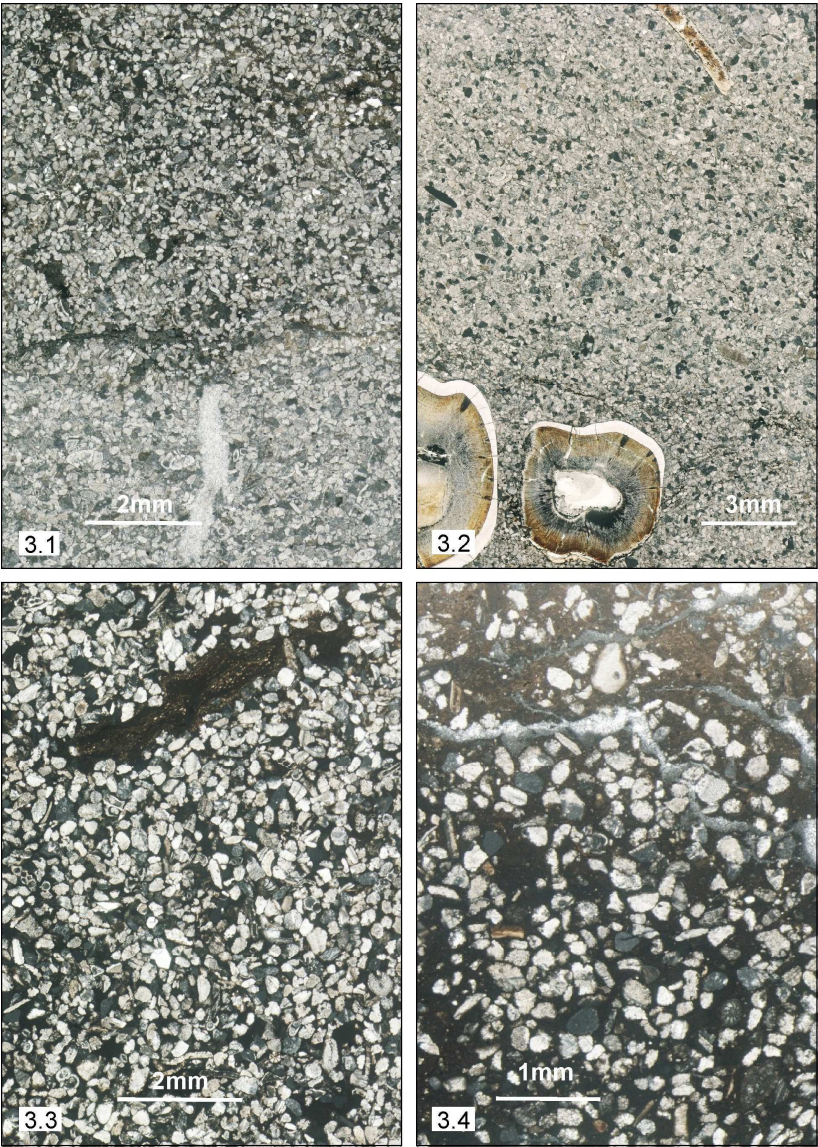


Figure 3.1. Scontrone Fossil Site section. Bioclastic packstone with large

*specimens of Ammonia (lower side) crossed by a vertical bifurcating spar-filled root mould. A dark irregular string marks the contact with the overlying eolian carbonate. Scontrone Member of the Lithothamnium Limestone, top of the **a** interval. 3.2. Scontrone Fossil Site section. Well-sorted litho-bioclastic packstone with well preserved vertebrate teeth (lower-left side) showing the characteristic brownish dentine surrounded by a thick rim of colourless enamel. In the upper-right side a vertebrate bone fragment is present. Scontrone Member of the Lithothamnium Limestone, top of the **a** interval. 3.3. Scontrone South-West section. Wind-blown marine biogenic detritus sparse in a dense pedogenic micrite matrix. Presence of sparse planktonic forams landward transported during storm events. A large dark-brown root (upper-central part) still retaining a perfectly preserved cellular structure at very high magnification. Scontrone Member of the Lithothamnium Limestone, top of the **a** interval. 3.4. Scontrone South-West section. Wind-blown biotritus associated with small rounded micrite grains set in a rubified pedogenic micrite. In the upper part of the picture, net of root traces and geopetally-filled syneresis cracks. Scontrone Member of the Lithothamnium Limestone, top of the **a** interval.*

regressive moment of the parasequence. The bulk of the Scontrone vertebrate remains have been recovered from this horizon (Fig. 3.2). The subaerial origin of the rubified calcarenite veneer is proven by the occurrence of large rhizoliths (Fig. 3.3) and by the presence of a close network of root traces (Fig. 3.4). A subaerial origin is also indicated by the abundance of medium to fine-sand-sized calcareous extraclasts associated with reworked and broken tests of planktonic and benthic foraminifers plus unidentified bioclasts. The presence of allochthonous material, the fauna derivation from different realms and the general conditions of the tests unequivocally attest eolian deposits accumulated by deflation processes on marine-derived materials. In conclusion, the results of the performed petrographic analysis show that the deposit yielding the Scontrone vertebrates is a wind-driven calcarenite draping the top of subtidal sand bars.

Modern eolian carbonates are common along arid to semiarid wind-

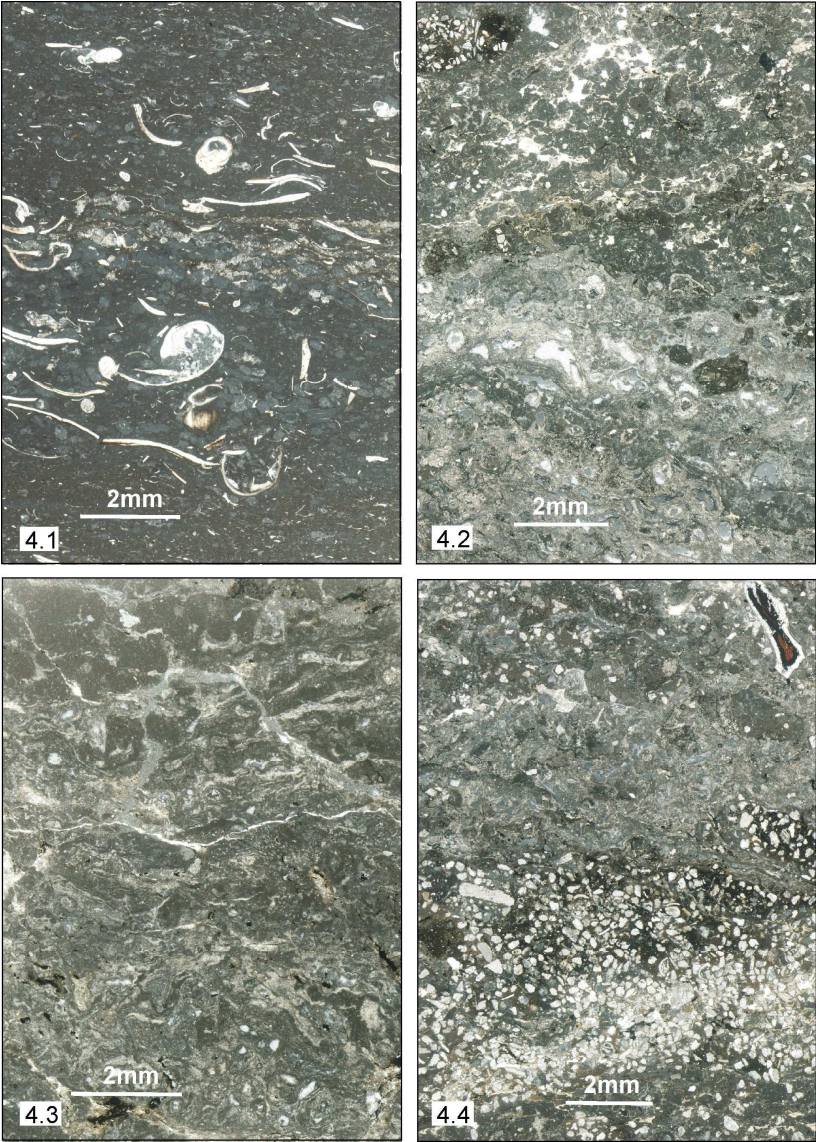


Figure 4.1. Scontrone South-West section. Wackestone with ostracods and

*hydrobiids associated with small micritized rounded grains mainly represented by coprolites (recognizable at high magnification). In the centre of the picture, lamina of coprolite-rich packstone. Scontrone Member of the Lithothamnium Limestone, marsh deposit of the **b** interval. 4.2. Scontrone Fossil Site section. Dark-brown to pale yellow mottled mudstone affected by intense pedogenic process. Circumgranular cracks (upper part of the picture) and calcified thick root mat with transverse and oblique sections of spar-filled root moulds (circular white hollows with grey micrite or microsparite centre). Scontrone Member of the Lithothamnium Limestone, marsh deposit of the **b** interval. 4.3. Scontrone South-West section. Dark-brown to pale yellow mottled mudstone affected by intense root activity and syneresis processes. Scontrone Member of the Lithothamnium Limestone, marsh deposit of the **b** interval. 4.4. Scontrone Fossil Site section. Colour mottled mudstone with flakes of rubified rooted eolianite crust. The groundmass is represented by a dense network of calcified root mat. At the upper right corner, worn fragment of vertebrate. Scontrone Member of the Lithothamnium Limestone, marsh deposit of the **b** interval.*

exposed coastlines located in wide carbonate-ramp settings with abundant calcareous-sand production.

The described eolian carbonates are overlain by grey-green to yellowish muddy deposits (interval **b** in the columnar sections) testifying to a sudden change in the environmental conditions with the establishment of intermittently flooded mudflats. These deposits are principally represented by Wackestones rich in small hydrobiids and dreissenids, ostracods and thick-walled *Ammonia* frequently associated with coprolites and charophyte gyrogonites (Fig. 4.1). The mudstones show a crude lamination and a grey-green to yellowish-green mottled appearance. The microscopic analysis shows that the vague, irregular lamination is related to the discontinuous presence of crinkled microbial laminae disrupted by root activity. The mottled appearance is related to the presence of yellowish to pinkish flakes of eolianite removed from the early-lithified wind-exposed substrate

and to the presence of syneresis cracks, well preserved calcified roots and small planar fenestrae (Figs. 4.2-4.4). Such features point to an intermittent exposure of the muddy sediment associated with intense pedogenesis. Interval **b** displays quite relevant changes in facies and thickness within a relatively small area and a rapid lateral pinch-out towards the east (Scontrone Fossil Site) and south (Scontrone South-West and Scontrone South sections). In the Sangro Gorge and Scontrone North sections, where the **b** interval reaches the maximum thickness (5 and 3 metres, respectively), the mudstones contain channelized pebbly deposits with lithoclasts derived from the substratum (Sangro Gorge) as well as brackish-water shell lag accumulations. The lowest shell bank, present in both sections, is characterized by winnowed, disarticulated and deeply bored oyster thick valves (Fig. 5.1). Cerithiids and potamidids dominate the lumachella layers in the upper portion of the **b** interval (Fig. 5.2). Desiccation cracks systematically affecting the top of the single lumachella layers (Figs. 5.3 and 5.4) and deep root penetration testify to short episodes of subaerial exposure. The facies analysis of the **b** interval indicates a muddy intertidal flat incised by ephemeral channels or small creeks in which lumachella lags and sporadic conglomerates were accumulated by strong tidal currents. The deeply rooted thin muddy deposits of the Scontrone Fossil Site and Scontrone South-West sections give evidence of well vegetated mud flats and marshes flanking the tidal creeks. In both sections the marsh muddy deposits contain scarce and badly preserved bone fragments (Figs. 4.2 and 4.4). In conclusion, the bulk of the Scontrone vertebrate remains are embedded in a rooted wind-blown calcarenite sealed by tidal-marsh muddy deposits containing rare and scattered bone fragments.

The upper parasequence is characterized by an upward increase in the sand/mud ratio associated with an increase in the thickness of the beds. The lower transgressive portion (interval **c**)

consists of tan foetid marls and shaly marls with thin intercalations

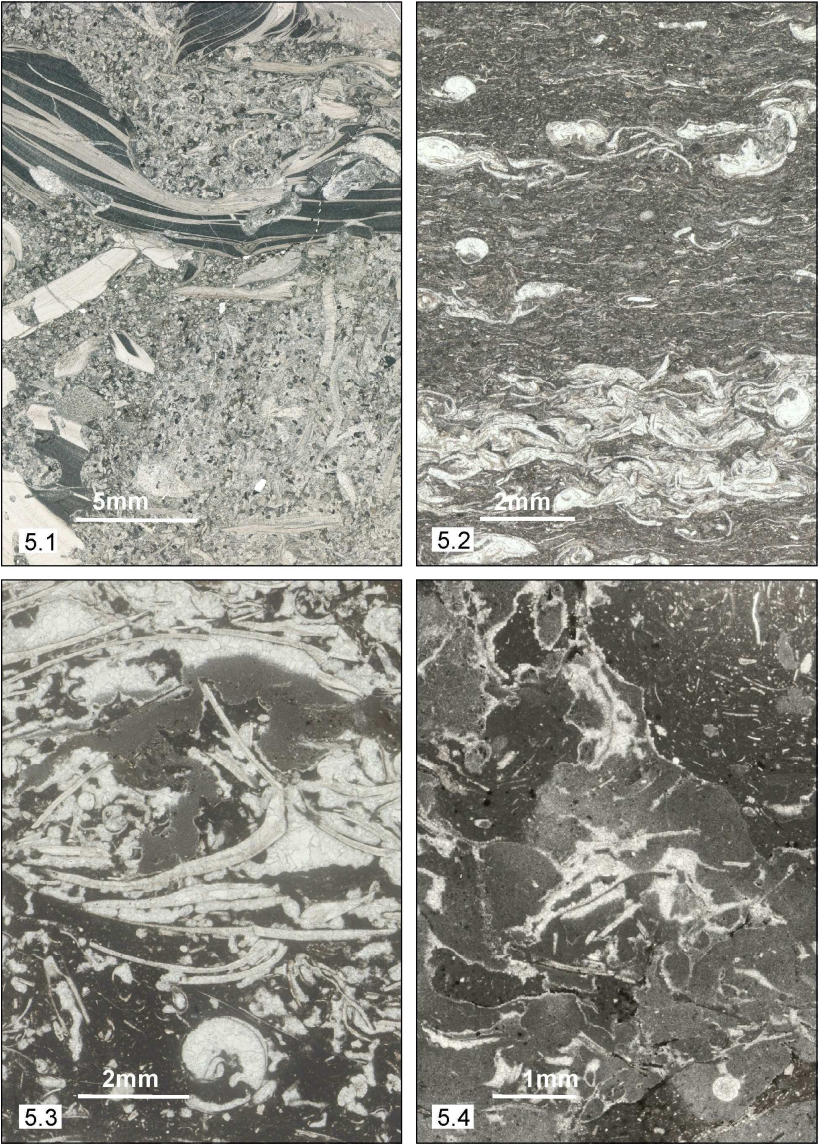


Figure 5.1. Scontrone North section. Fine-grained bioclastic packstone with

fragmented and deeply bored oyster shells. Scontrone Member of the Lithothamnium Limestone, lower portion of the b interval. 5.2. Scontrone North section. Densely packed gastropod-rich lumachella layer with flattened and crushed shells of hydrobiids. The background sediment is represented by a packstone with thin-walled disarticulated ostracods. Scontrone Member of the Lithothamnium Limestone, Bioclastic accumulation of a subtidal marsh deposit. 5.3. and 5.4. Sangro Gorge section Lumachella layer showing large geopetally-filled vugs and cracks. Scontrone Member of the Lithothamnium Limestone, desiccated and brecciated top of the gastropod-rich lumachella layer.

of brackish-water lumachella beds made up of flattened complete shells of potamidids and cerithiids with a high percentage of thick-walled *Ammonia*, ostracods and sparse *Elphidium* (Fig. 6.1). These mud-dominated transgressive deposits include fine to medium-grained grey litho-bioclastic calcarenites characterized by ripple laminations within medium-scale trough sets which have been interpreted as storm layers accumulated in a coastal lagoon. These bio-lithoclastic calcarenites, composed of a fine-grained biodetritus (echinoid spines, serpulid and barnacle debris associated with *Ammonia* and *Elphidium*), show frequent lag accumulations of fragmented cerithiids and sparse disarticulated oyster shells. Small fragments of vertebrates have been found in the lowest channelled calcarenite. Interval c reaches the maximum thickness in the Sangro Gorge and Scontrone North sections (around 2.50 metres) and rapidly thins moving towards the east and the south. In the Scontrone South-West section it is represented by 1.5 metres of thinly laminated tan foetid marls and shaly marls the lower portion of which is rich in *Dreissena*, *Melanopsis* and hydrobiids testifying to hypohaline water conditions. In thin section the marls show calcisphaerulid-rich laminae (Fig. 6.2) probably representing blooms of calcareous resting cysts of algae or calcitized sporomorphs. In the

Sangro Gorge the uppermost portion of the c interval is represented by more open lagoon deposits as indicated by the presence of sparse

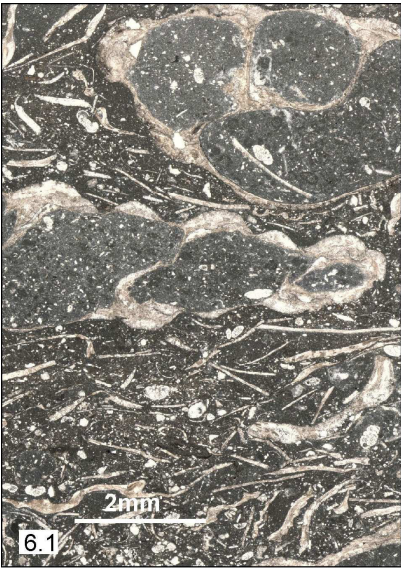


Figure 6.1. *Scontrone North section. Bioclastic wackestone/packstone with crushed cerithiids, large-sized Ammonia and ostracods. Scontrone Member of the Lithothamnium Limestone, c interval, storm accumulation in a brackish-water lagoon. 6.2. Scontrone South-West section. Very fine-grained bioclastic packstone with calcisphaerulid-rich laminae (white spots mainly concentrated in the upper part of the picture). Disarticulated valves of dreissenids. Scontrone Member of the Lithothamnium Limestone, c interval, inner-lagoon deposit with oligohaline to hypohaline water. 6.3 and 6.4. Scontrone North section (6.3) and Scontrone South section (6.4.). Very well-sorted fine-grained bio-lithoclastic grainstone with oversized well-rounded calcareous clasts. Scontrone Member of the Lithothamnium Limestone, tidal bar deposit of the d interval.*

cardiids together with the cerithiids. A change into slightly saltier waters, up to mesohaline conditions is also suggested by the occurrence of oyster shell lags accumulated in shallow tidal channels near the top of the interval (see Scontrone Fossil Site).

The **d** interval, well exposed in the Sangro Gorge and Scontrone South sections, is principally composed of off-white medium-grained litho-bioclastic calcarenites (Fig. 6.3) with a biogenic content characterized by euryhaline and stenohaline fossil associations. These calcarenites consist of well sorted bioclastic grainstones with sparse oversized, very well rounded and locally bored calcareous clasts (Figs. 6.3 and 6.4) and with thick-walled gastropods. Low-angle cross stratification is locally present, but usually it has been shaded by the intense bioturbation. Discontinuous layers of thick-walled oysters occur at the base of the calcarenite beds. These deposits making the bulk of the **d** interval have been interpreted as thick sand-bar accumulations in proximity to higher-energy settings and more open coastal environments. In the Scontrone South section the top of the interval is marked by a thin layer of extensively rooted fine-grained calcarenite in which

vertically elongated root tubules have been filled with dark organic material. The high-energy sand-bar deposits are overlain by 1.5 metres of lagoon deposits mainly represented by thinly laminated

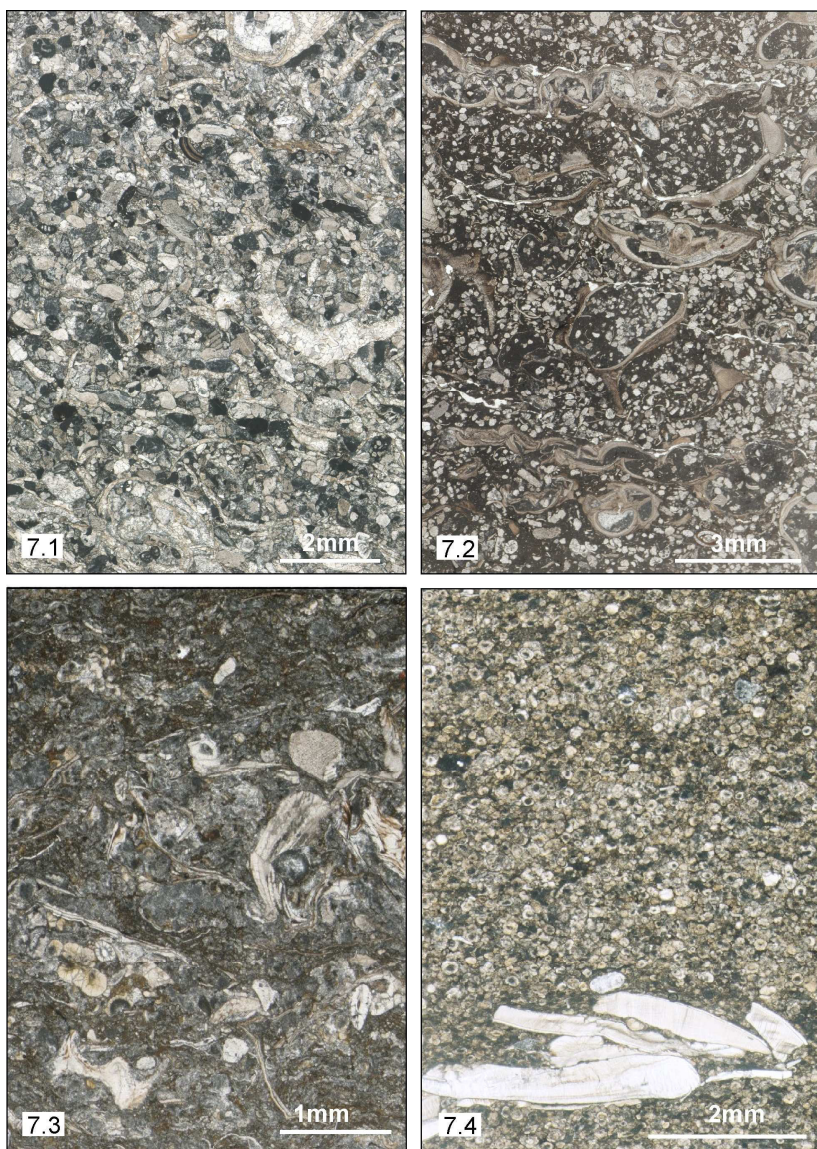


Figure 7.1. Scontrone South-West section. Bio-lithoclastic packstone with well-rounded biogenic and lithic grains. In the left side, transversal section

*of spar-filled thick-walled gastropods. Scontrone Member of the Lithothamnium Limestone, tidal bar deposit of the **d** interval. 7.2. Crushed cerithiids preserving their original aragonite shell in a fine-grained bioclastic wackestone/packstone rich in Ammonia. Sangro Gorge section. Scontrone Member of the Lithothamnium Limestone, top of the **d** interval, storm layer accumulated in a coastal lagoon. 7.3. Scontrone South section. Bioclastic packstone with fragmented shells. In the lower-left side of the picture, yellow cluster of calcareous resting cysts of algae or calcitized sporomorphs. Immediately above the yellow cluster, well-preserved white dehiscent cysts. Scontrone Member of the Lithothamnium Limestone, top of the **d** interval, restricted inner part of a coastal lagoon. 7.4. Scontrone South section. Densely packed calcisphaerulid packstone with crushed shell fragments of cerithiids. The exceptional abundance of these spherical calcareous bodies may be related to a phytoplankton bloom in waters with high level of eutrophication. Scontrone Member of the Lithothamnium Limestone, top of the **d** interval, restricted coastal lagoon.*

foetid marls and shaly marls rich in potamidids and cerithiids (Fig. 7.2). In the Scontrone South section the lagoon deposits overlying the rooted dark surface of the sandbar calcarenite are represented by dark shaly marls and limey marls containing scattered micritized bioclasts, crushed potamidids, cerithiids and dreissenids together with plant remains and numerous thick-walled ostracods. At high magnification the shaly marls reveal the presence of numerous spherical to ovoidal calcareous bodies (Fig. 6.3.) likely representing intact or partly dehiscent calcareous resting cysts of algae or calcitized sporomorphs. A thin bed (30 centimetres) of foetid dark-brown calcisiltite with a characteristic microscopic fabric (Fig. 7.4) is present at about 20 cm from the base of the muddy lagoon deposits. In thin section the calcisiltites appear as a dense aggregate of calcareous microspheres representing an unusual in situ accumulation of algal cysts or calcitized sporomorphs in the protected innermost part of the lagoon. The return to protected

lagoon conditions after the high-energy sand-bar deposition attests the shoaling-up facies architecture of the second parasequence.

In the Scontrone South section the second parasequence is clearly truncated by the erosional surface at the base of the shallow-marine offshore bars. The basal portion of the high-energy sandbars consists everywhere of medium to coarse-grained litho-bioclastic calcarenites with a grain-supported fabric and a fossil association characterized by abundant stenohaline organisms (echinoid spines, fragmented barnacles, scattered coralline algal rhodoids and *Ammonia*, together with large sized *Elphidium* and fragmented *Heterostegina* probably displaced by storms).

Stop illustration

Stop 1. Sangro Gorge

See figures 8 and 9 and foldout 2



Figure 8. Panoramic view on the Sangro Gorge stratigraphic section.

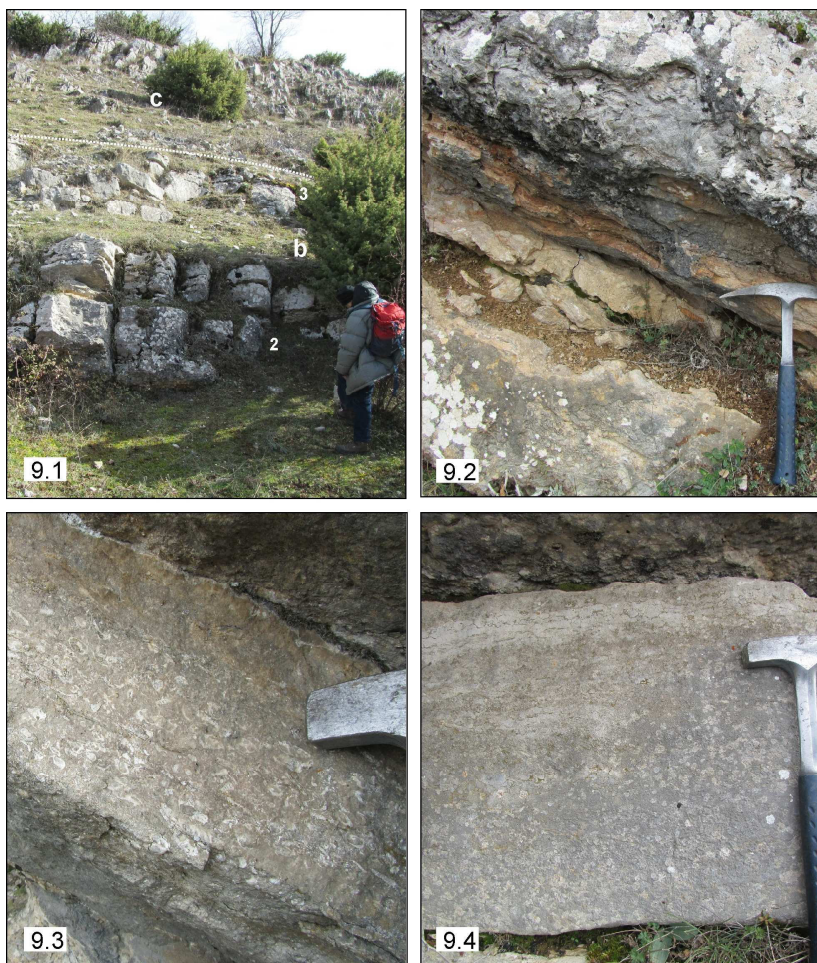


Figure 9. Sangro Gorge section. Tidal channel deposit in the regressive tract of the lower parasequence of the Scontrone Member (interval **b**). **9.1.** Channelized beds (2 and 3 in the picture overlain by lagoon deposits of the **c** interval. Note the evident concave-up lower surface of the channel deposit 2. **9.2.** Enlarged view of the upper part of the channel deposit 2 with a very thick oyster shell-bed. **9.3.** Enlarged view of the cerithiid shell lag

accumulation in correspondence to the tidal channel 3. **9.4.** Tidal channel topped (above the head of the hammer) by a mudstone with evident desiccation structures.

Stop 2. Scontrone Fossil Site

See figure10 and foldout 2

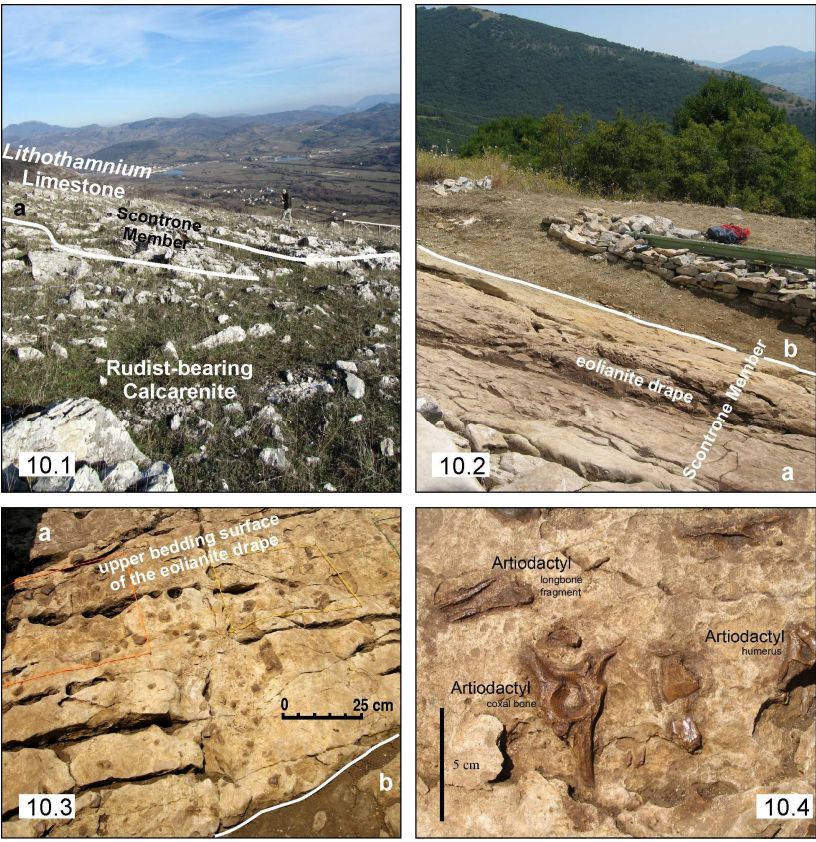


Figure 10. Scontrone Fossil Site. **10.1.** Panoramic view of the contact between the Albian-Turonian basinal Rudist-bearing Calcarene and the

*Tortonian ramp carbonates of the Scontrone Member of the Lithothamnium Limestone. 10.2. Eolian calcarenite drape (top of the lower parasequence) containing the bulk of the vertebrate remains (top of the **a** interval) and contact with the overlying muddy marsh deposit. 10.3 and 10.4. Upper surface of the eolianite deposits with vertebrate remains.*

Stop 3. Scontrone South

See figures 11 and 12 and foldout 2

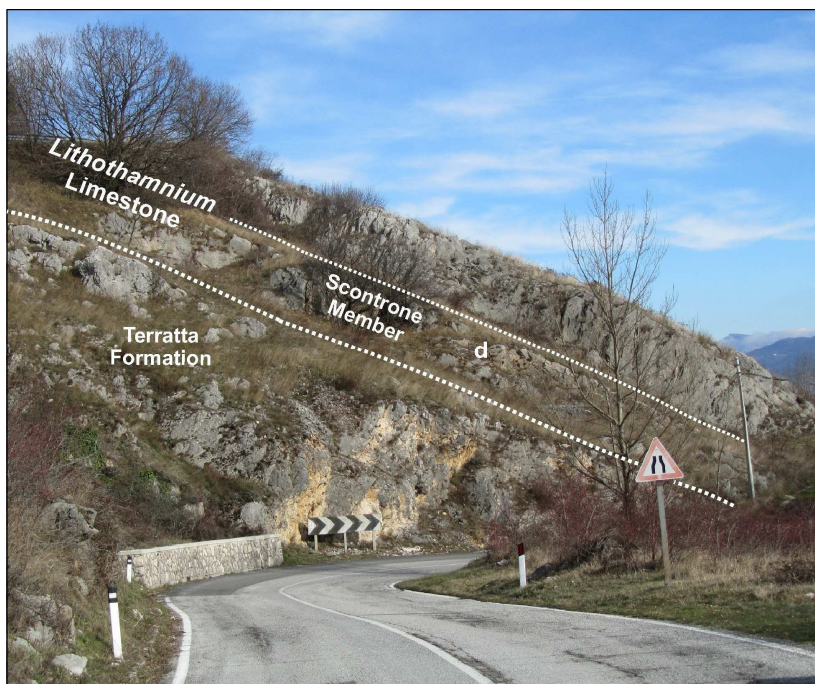


Figure 11. *Scontrone South section. Second parasequence of the Scontrone Member (**d** and **e** intervals) directly overlying the Neocomian-Barremian platform-edge deposits of the Terratta Formation.*



Figure 12. Details of the Scontrone South section. **12.1.** Tidal bar calcarenite (**d**) belonging to the transgressive tract of the second parasequence of the Scontrone Member unconformably overlying the Terratta Formation. **12.2.** Lagoon deposits belonging to the regressive tract of the second parasequence overlain by shallow-marine calcarenites. The

contact corresponds to an erosional surface. **12.3.** Top of the tidal-bar calcarenite showing large-scale and low-angle cross stratification. Transgressive tract of the second parasequence (interval **d**). **12.4.** Close-up view of the intensively rooted upper surface of the tidal-bar calcarenite of figure 12.3 displaying thin vertical tubules filled with dark organic materials.

Stop 4. Scontrone Cemetery

See figure 13 and foldout 2



Figure 13. Scontrone Cemetery section. Unconformable contact between the Lithothamnium Limestone and the Rudist-bearing Calcarenite.

Dipartimento di Scienze della Terra e Museo di Storia Naturale, Sezione di
Geologia e Paleontologia
Università degli Studi Firenze

The richly fossiliferous bonebed was discovered in 1990, when a ranger of the National Park of Abruzzo showed some bone fragments to two researchers of the University of Florence, P. Mazza and M. Rustioni, who were then studying bears. The site is located on the eastern side of the Civita Mountain, some 1180 m above sea level. Since discovery, excavations have been conducted on a yearly basis up to the end of the last century.

The collection of mammalian remains, which are preserved at the Centro di Documentazione Paleontologico at Scontone, consists, at the moment, of over 80 reptile remains, and almost 500 mammal bones, which include at least 3 specimens of the giant moonrat *Deinogalerix*, as well as 470 artiodactyl bones (22 cranial and maxillary bone fragments, 39 mandibles, 114 isolated cheek teeth, 153 postcranial bones, 142 indeterminate specimens) all belonging to the bizarre ruminant *Hoplitomeryx*. The analysis of the artiodactyls enabled the identification of several different dental, cranial and jawbone morphotypes. At the moment, *Hoplitomeryx* is monospecific, being represented by the only *H. matthei*, which was created by Leinders (1983) on Gargano fossil material. The reconstructed skull of *H. matthei* is five-horned, has a short muzzle, semi-stereoscopic orbits, and two long, sabre-like upper canines. Unfortunately, Leinders (1983) failed to describe the teeth and limb bones of these animals. He classified the Hoplitomerycidae among

the Cervoidea, but this opinion is not shared by some authors (Mazza & Rustioni, 1996; Hassanin & Douzery, 2003).

A fragmental right maxillary of moorat with associated M3 and the postero-lingual portion of M2, was found in 1999. It proved the presence of *Deinogalerix freudenthali* (Mazza & Rustioni, 2008). Some even larger moonrat remains were freed from the calcarenites of the Scontrone member; their analysis is under way.

The area exposed at the site is divided obliquely into three separate zones, which correspond to three stratigraphically superimposed bone-bearing layers. The lowest term is a grey biocalcarene which outcrops at the upper left: it contains only rare and heavily weathered bone fragments. The second layer is a stripe which crops out from the lower left to the upper right of the exposed area. This is a calcarenite with yellowish nodules, very rich in root casts. This is where the vertebrate remains are most abundant and better preserved. Numerous bone fragments and a few isolated teeth of artiodactyls and crocodiles are visible, but the bone collection of this layer is largely dominated by fragments of marsh turtle carapax. The third layer, a nodular calcilutite, contains a lower amount bones comparatively worse preserved than those of the underlying level.

The bones are well fossilized, but most are broken. They are all disarticulated, unsorted and randomly scattered in every layer. None shows evidence of reworking: all are fossilized in ferric oxides, and lack characteristic signs of transport, i.e. abrasion, or polishing. In the collection of bones hitherto collected at Scontrone, the percentage of Korth's (1979) settling groups, which are practically a re-calibration of the Voorhies (1969) Groups for small mammals, is consistent with the value of Behrensmeyer's (1975) tooth/vertebra ratio. The best represented bones at Scontrone are those of Korth's (1979) groups II (skull, scapula, molars, femur, astragalus), and II & III (mandible), which indicate a possible lag deposit, formed by elements gradually

removed which are dragged, or just flip over, remaining basically associated with the substratum during transport. Behrensmeyer's (1975) tooth/vertebra ratio is high, 11.37, due to the comparatively large amount of isolated teeth, which are dense, lag elements. The co-occurrence of the land mammal elements, shattered marsh turtle carapax portions and teeth and sparse ossicles of crocodile implies that the bone amassment consists of elements of animals possibly mired in, or near, a marsh or coastal lagoon (Weigelt, 1989), whose skeletons were dissected and scattered by tides and/or storms. The chronological constraints of these contexts indicate that Scontrone must be a time-averaged bone accumulation. Because of the low sedimentation rates in marshes and/or coastal lagoons [time intervals of 10^3 years according to Hope (2002) and Suprin & Hope (2001)], carcasses lie exposed on the substratum long enough to be thoroughly skeletonized and disarticulated. Tidal currents can easily select the isolated bones, readily removing the lightest ones. Hence, the accumulation of a sizeable amount of bones in slowly depositing marshes necessarily requires a considerable lapse of time.

References

- BEHRENSMEYER A. (1975) - The taphonomy and paleoecology of Plio-Pleistocene vertebrate assemblages east of Lake Rudolf, Kenya. *Bulletin of the Museum of Comparative Zoology*, 146: 473-578.
- HASSANIN A. & DOUZERY E.J.P. (2003) - Molecular and Morphological Phylogenies of Ruminantia and the Alternative Position of the Moschidae. *Systematic Biology*, 52: 206-228.
- HOPE G.S. (2002) - The Late Quaternary of Kiritimati (Christmas) Island, Kiribati. In ANDERSON A., MARTINSSON WALLIN H. & WALLIN P. (Eds.), *The Prehistory of Kiritimati (Christmas) Island, Republic of Kiribati*

- Excavations and analyses. *Kon-Tiki Museum Occasional papers*, 111-118.
- KORTH W.W. (1979) - Taphonomy of microvertebrate fossil assemblages. *Annals of the Carnegie Museum*, 48: 235-285.
- LEINDERS J. (1983) - Hoplitomerycidae fam. nov. (Ruminantia, Mammalia) from Neogene fissure fillings in Gargano (Italy). Part. 1: The cranial osteology of Hoplitomeryx gen. nov. and discussion on the classification of pecoran families. *Scripta Geologica*, 70: 1-68.
- MAZZA P. & RUSTIONI M. (1996) - The Turolian fossil artiodactyls from Scontrone (Abruzzo, Central Italy) and their paleoecological and paleogeographical implications. *Bollettino della Società Paleontologica Italiana*, 35: 93-106.
- SUPRIN B. & HOPE G.S. (2001) - A Pleistocene record of *Neocallitropsis pancheri* (Cupressaceae) from the Plaine des Lacs, New Caledonia. *Quaternary Australasia*, 19: 17-21.
- VOORHIES M. (1969) - Taphonomy and population dynamics of an early Pliocene vertebrate fauna, Knox County, Nebraska. *University of Wyoming Contributions to Geology, Special Paper* 1: 1-69.
- WEIGELT J. (1989) - *Recent Vertebrate Carcasses and Their Paleobiological Implications*. University of Chicago Press, Chicago.

Excursion 2: Palena and Majella, 5th March 2011.

46

Dipartimento di Scienze della Terra, Università di Pisa

The Montagna della Majella is an arc-shaped anticline trending NW-SE in the north and NNE-SSW in the south, made up of Mesozoic-Tertiary carbonates overlain by Messinian evaporites and marls followed by lower Pliocene siliciclastic flysch deposits (Fig. 1). In the north, the Majella Unit is tectonically covered with a by closely folded Messinian-lower Pliocene siliciclastic flysch deposits belonging to the Queglia Unit, a nappe occupying in the Apenninic edifice an intermediate position between the Majella and the Morrone-Porrara units. The northern termination of Majella beneath the Queglia Unit follows the periclinal closure of the structure controlled by the gentle plunging of the fold axis towards the NW. The southern termination, controlled by an axial plunging towards SSW, is less regular because of the occurrence of extensional faults which have re-utilized the previous thrust surface of the Morrone-Porrara Unit over Majella (see Fig. 2). Along the eastern flank of the anticline, which dips regularly towards the east (Fig. 3), basin-derived allochthonous sheets (Molise Nappes) tectonically lie over the Pliocene flysch of Majella.

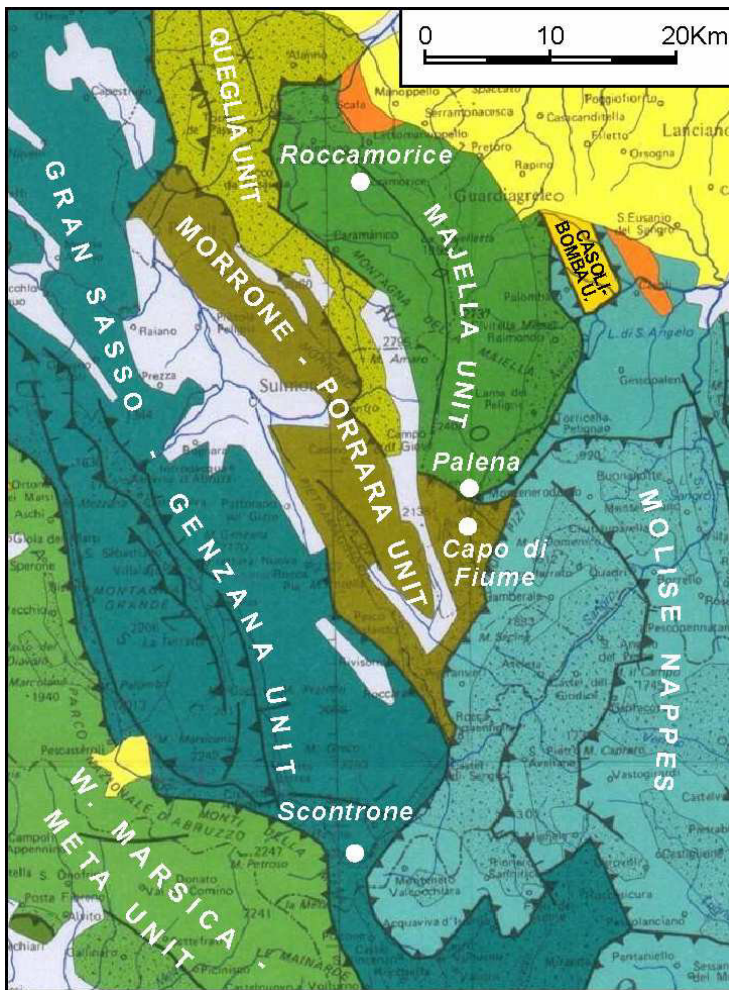


Figure 1. Simplified geological-structural map of the Majella and surrounding areas showing the areal distribution of the recognized tectonic units. In the different tectonic units dots indicate siliciclastic flysch deposits. Orange indicates Pliocene thrust-top deposits while yellow indicates Pleistocene deposits post-dating the nappe transport. Modified after Patacca & Scandone (2007).



Figure 2. Panoramic view on the southern Majella and Porrara mountains. Serra Campanile is a splay of the Porrara thrust sheet. The thrust contact between Serra Campanile and Majella has been re-mobilized by low-angle normal faulting during the uplift of Majella. The picture also indicates the location of three sections (Capo di Fiume, Palena Cemetery and Vallone di Taranta) visited during the excursion.



Figure 3. Detail of figure 2 showing the east-dipping carbonates (mostly Tertiary carbonates) in the regular eastern flank of the Majella anticline. Pliocene siliciclastic flysch deposits crop out in correspondence to the green meadow in the right hand of the picture. Palena lies on thrust-top deposits unconformably covering the Molise Nappes.

The western margin of Majella coincides with a system of normal faults (Caramanico Fault System) displaying a maximum cumulative downthrow that exceeds 3500 metres. This fault system has been interpreted as a gravity-collapse feature that has progressively accommodated with a listric geometry the increase in the structural elevation created by a backthrust structure grown in the footwall of the Majella anticline (Patacca et al., 2008). In correspondence to the fold axis culmination, the Majella carbonates are spectacularly exposed in peaks exceeding 2700 metres in elevation (Fig. 4).



Figure 4. Panoramic view of the Majella Mountain from west. A Lower Cretaceous-Lower Miocene section of shallow-water carbonates is exposed at Monte Amaro (2793 metres a.s.l.). A platform-to-basin transition is preserved in correspondence to Pesco Falcone. The Caramanico Fault System, highlighted by the tree line in the right hand of the picture, runs at the foot of the Mesozoic-Tertiary carbonates and its downthrow decreases considerably moving from Monte Amaro (more than 3000 metres) to La Rapina (about 1000 metres).

As concerns the facies of the Mesozoic deposits, Berriasian-Campanian shallow-water limestones crop out in the Southern Majella area whilst Aptian-Campanian basinal deposits characterize the Northern Majella area. In addition, subsurface data show that in the northernmost area basinal conditions started from the middle/upper Liassic (Musellaro 1 well). A Cretaceous platform-to-basin transition is spectacularly exposed in Central Majella

(Crescenti et al., 1969; Accarie, 1988; Vecsei, 1991; Eberli et al., 1993; Morsilli et al., 2002; see Fig. 5).

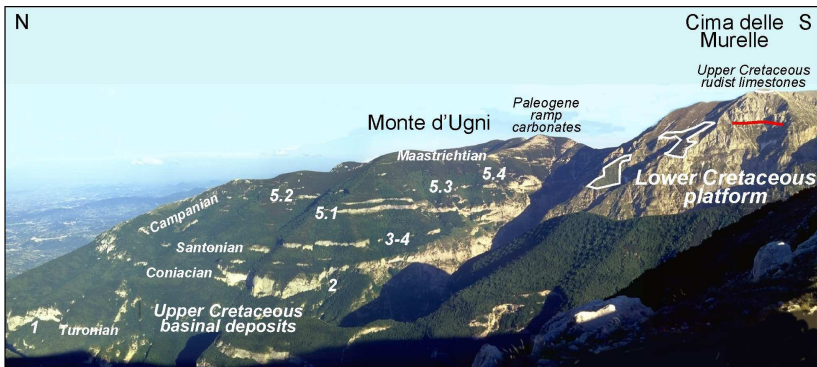


Figure 5. Panoramic view on the Upper Cretaceous paleoslope of Central Majella showing Turonian-Campanian onlapping breccias that progressively fill the proximal basinal areas. Arabic numerals indicate the principal breccia bodies, the stratigraphic position of which is given in foldout 3 of this guidebook. Note the gradual decrease in the clinostratification of the breccias moving from the Turonian breccia 1 to the Campanian breccia 5. Irregular white polygons indicate outcrops of hemipelagic limestones (Scaglia Formation) draping the paleoslope. Starting from Maastrichtian, a ramp physiography substituted the previous slope-to-basin configuration allowing a northward progradation of Maastrichtian and Paleogene shallow-water carbonates.

In this sector, a segment of the Upper Cretaceous paleoslope limiting in the north the carbonate platform is very well preserved with talus breccias that progressively filled the proximal areas of the basin allowing in the Maastrichtian the northward progradation of coarse-grained ramp calcarenites. A chronostratigraphic scheme of the Mesozoic-Tertiary deposits of the Majella Mountain along an ideal N-S section is provided in foldout 3 of this guidebook.

A comparable platform-to-basin transition is also known in the Mesozoic carbonates of the Morrone-Porrara Unit, with basinal facies developed in north-western Mt. Morrone and platform facies developed in south-eastern Mt. Morrone and in Mt. Porrara. Exposures, however, are not so beautiful as in Majella.

References

- ACCARIE H. (1988) – Dynamique sédimentaire et structurale au passage plate-forme/bassin. Les faciès carbonatés crétacés et tertiaires du Massif de la Maiella (Abruzzes, Italie). *Ecole des Mines de Paris, Mémoires de Sciences de la Terre*, 5: 1-162.
- CRESCENTI U., CROSTELLA A., DONZELLI G. & RAFFI G. (1969) – Stratigrafia della serie calcarea dal Lias al Miocene nella regione marchigiano-abruzzese. (Parte II. Litostratigrafia, Biostratigrafia, Paleogeografia). *Memorie della Società Geologica Italiana*, 8: 343-420.
- EBERLI G.P., BERNOULLI D., SANDERS D. & VECSEI A. (1993) – From aggradation to progradation: the Maiella platform, Abruzzi, Italy. In SIMO T., SCOTT R.W. & MASSE J.P. (Eds), Cretaceous Carbonate Platforms. *Memoirs of the American Association of Petroleum Geologists*, 56: 213-232.
- MORSILLI M., RUSCIADELLI G. & BOSELLINI A. (2002) – Large-scale gravity-driven structures: control on margin architecture and related deposits of a Cretaceous carbonate platform (Montagna della Maiella, Central Apennines, Italy). *Bollettino della Società Geologica Italiana*, Special Issue 1: 619-628.
- PATACCA E., SCANDONE P., DI LUZIO E., CAVINATO G.P. & PAROTTO M. (2008) – Structural architecture of the central Apennines: Interpretation of the CROP 11 seismic profile

from the Adriatic coast to the orographic divide. *Tectonics*, 27: TC3006, doi: 10.1029/2005TC001917.

VECSEI A. (1991) - *Aggradation und Progradation eines Karbonatplattform-Randes: Kreide bis Mittleres Tertiär der Montagna della Maiella, Abruzzan*. Mitteilungen aus dem Geologischen Institut der Eidgenössischen Technischen Hochschule und der Universität Zürich, Neue Folge, nr. 294.

THE CAPO DI FIUME STRATIGRAPHIC SECTION

Giorgio CARNEVALE*, Etta PATACCA** & Paolo SCANDONE**

*Dipartimento di Scienze della Terra. Università degli Studi di Torino

**Dipartimento di Scienze della Terra. Università di Pisa

The Capo di Fiume stratigraphic section (Figs. 1, 2.1) has been discussed by many authors (e.g., Bellatalla et al., 1992; Carboni et al., 1992; Patacca et al., 1992; Mazza et al., 1995; Miccadei & Parotto, 1998; Carnevale, 2003) who have described its lithological and paleontological features with different degrees of detail. The section is composed of paralic to open marine mud-dominated Messinian deposits overlying a relatively thick “terra rossa” horizon attesting to a prolonged subaerial exposure. The “terra rossa” soil covers uppermost Cretaceous limestones, but a minor fault has locally obliterated the original stratigraphic contact.

The Cretaceous carbonates below the “terra rossa” deposits consist of medium-grained bioclastic limestones characterized by a pseudo-crystalline texture which explains the name given to this lithostratigraphic unit (Saccharoidal Limestone). Actually, the saccharoidal aspect derives from the nature of the bioturbation almost exclusively composed of abraded and worn *Inoceramus* prisms, echinoid spines and *Pithonella*-like calcisphaerulids. Large scale low-angle planar cross stratification with bidirectional dip (Fig. 2.2) points to offshore marine bars in a ramp-like open-shelf setting. The top of the Saccharoidal Limestone is characterized in the last 10-15 centimetres by a strong bioturbation, expressed by horizontal and oblique large burrows (Fig. 3.1) suggesting a nearshore stressed

environment. The groundmass of the overlying red-stained illuvial soil consists of a fine mixture of red to yellow clay minerals, Fe and Fe/Mn hydroxides, unstained silty-sized eolian quartz-grains and scarce mica flakes. The groundmass also includes isolated and

massive muddy deposit emplaced by mass-flow mechanism; 8, diatomitic marls; 9, "terra rossa" soil.

coalesced calcareous nodules, fine to medium-sand-sized subangular/subrounded carbonate lithoclasts with leached rims, locally abundant ferruginous pisoids and subordinate medium-sand-sized volcanic quartz and calcitized feldspars. The calcareous nodules consist of speckled micrite/microsparite masses precipitated in a vadose zone, frequently surrounded by an iron-enriched clayey red rim. Spar-filled circumgranular shrinkage cracks and complex networks of carbonate rhizoliths are the most common pedofeatures (Figs. 3.2 and 3.3). At places, porosities associated with root activities are partly or totally filled with well-preserved needle-fiber or whisker calcite cement of vadose origin (Fig. 3.4). The Messinian transgressive deposits overlying the "terra rossa" soil are organized into a deepening-up muddy sequence indicative of wetland to estuarine environments (a-c intervals in fig. 1, representing an equivalent of the *Lithothamnium* Limestone Formation), which evolves upwards into an open-marine shelf sequence (diatom-rich deposits representing an equivalent of the Tripoli Formation, see fig. 4.1). The lower portion of the sequence consists of paralic deposits represented by about 1.5 metres of grey to dark-brown mottled marls and clayey marls with very thin, lenticular beds of pebbly conglomerates (interval a in Fig. 1 and in Figs. 4.2 and 5.1). The pebbles of the conglomerates, characterized by pendant lower coats of white micritic chalky calcite are mainly composed of lower Cretaceous shallow-water limestones referable to a protected inner platform. Bahamian-type protected platforms were widely represented in the central-southern Apennine domains during the early Cretaceous. The marls, almost barren, consist of a micrite-sized pedogenetic carbonate with dispersed organic particles, clay minerals, fine to very fine sand-sized angular quartz grains and subangular to subrounded calcareous lithoclasts. The pedogenic

nature of these marls is also testified by the common occurrence of vadose whisker calcite inside vugs and cavities created by root



activity.

Figure 2.1. General view of the Capo di Fiume stratigraphic section. The white arrow points to the “terra rossa” soil. **2.2.** Capo di Fiume stratigraphic section. The “terra rossa” soil overlies upper Cretaceous ramp carbonated belonging to the Saccharoidal Limestone Formation. The white arrow indicates large-scale low-angle cross-stratification (emphasized by line drawing). The “terra rossa” soil is in turn overlain by Messinian deposits representing the equivalents of the upper portion of the Lithothamnium Limestone Formation and of the entire Tripoli Formation.

White lines mark stratigraphic contacts between the different lithostratigraphic units.

The mottled appearance is actually related to the presence of a faint network of subtle root tubules stained by dispersed organic particles or filled with black microaggregates of pyrite framboids (Figs. 6.1 and 6.2), as well as to the occurrence of light-coloured carbonate rhizoliths (Figs. 6.2 and 6.3). The dark colour, the pyrite concentration, the pervasive root burrowing and the common occurrence of circumgranular cracks (Figs. 6.2 and 6.3) are all hydromorphic features indicating a moist soil formed in a humid, strongly reducing environment in which long periods of saturation allowing Fe mobility alternated with periods of intense drying causing Fe concentration. The uppermost portion of interval **a** (Fig. 5.1 above the conglomerate) is constituted of grey marly clays alternating with organic-rich black shales containing plant remains and rare fragmented shells of *Vitrea* (terrestrial pulmonate gastropod of the *Zonitidae* family, see also Carboni et al., 1992).

The **a** interval grades upwards into about 50 cm of fissile and foetid dark-grey marls and shaly marls commonly assuming a whitish colour on weathered surfaces (**b** interval in Fig.1; see also Figs. 4.2, 5.1 and 5.2). The shaly marls are characterized by thin lumachella layers made up of a species-poor assemblage of aquatic or strongly hygrophilous land gastropods referable to ellobiids (*Carychium*), lymneids (*Lymnaea*) hydrobiids and vertiginids, associated with ostracods. The gastropods are indicative of stagnant freshwater ponds (*Lymnaea*), of brackish-water environments with salinity fluctuating from hypohaline to oligohaline conditions (hydrobiids) and of a humid densely vegetated land (*Carychium* and vertiginids). In the lower portion of the **b** interval the shell marls alternate with dark-brown to black euxinic layers rich in wood fragments displaying lighter current-driven wavy to lenticular detrital laminae (Fig. 6.4) composed of bioclastic ash, silt-sized

quartz grains, diffuse organic particles, sporomorphs and very fine sand-sized calcareous lithoclasts with well-rounded shape.

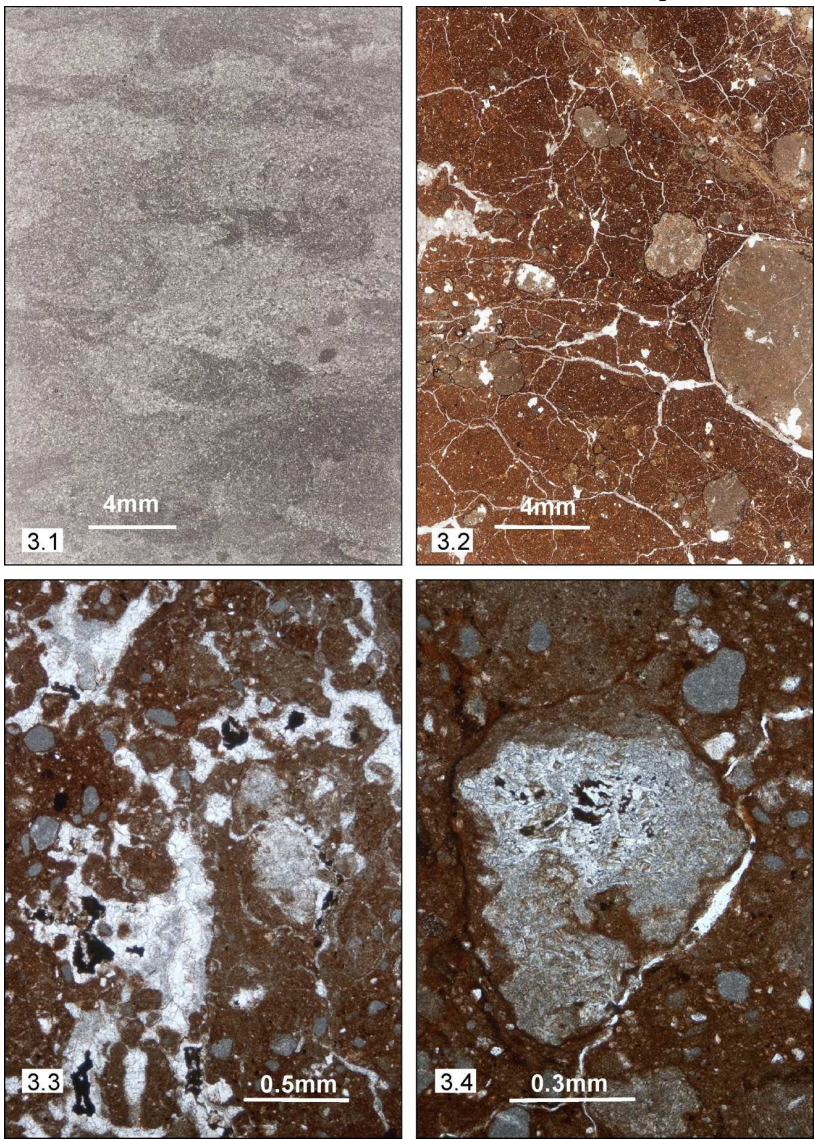
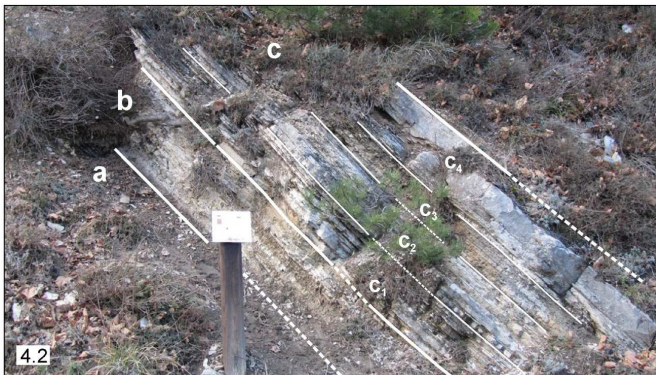


Figure 3.1. *Striated to oblique burrows at the top of the upper Cretaceous Saccharoidal Limestone. 3.2. "Terra rossa" soil. Spar-filled shrinkage cracks and carbonate nodules. In the left side of the picture, cluster of small nodules coated by a red rim of iron-enriched aluminous clays. 3.3. "Terra rossa" soil. Compound pedofeature consisting of spar and microspar-filled root channels and tubules (root residues still visible as black patches) crossed by a spar-filled discontinuous subtle network of syneresis cracks. Small calcareous lithoclasts are dispersed in the groundmass. 3.4. "Terra*

rossa" soil. Vugs partially filled with vadose "whisker calcite" cement. The central porosity has been loosely occluded by a coarse meshwork of calcite crystal laths.

Figure 4.1. Capo di Fiume stratigraphic section. The picture shows the stratigraphic contact between Messinian paralic deposits equivalent to the upper portion of the Lithothamnium Limestone Formation and marine deposits equivalent to the Tripoli Formation. **d₁** and **d₂** are diatomitic levels (same label as in figure 1). **4.2.** Capo di Fiume stratigraphic section.



Enlarged view of the Messinian deposits equivalent to the upper portion of the Lithothamnium Limestone Formation.

a: top of anoxic freshwater marsh deposits; b: foetid thinly laminated swamp deposits; c: brackish-water estuarine calcareous muddy deposits. Labels c₁-c₄ indicate the lithologic intervals separated in figure 1 and described in the text.

Both molluscs and lithofacies indicate a permanently flooded area in highly vegetated wetlands temporarily subject to feeble oscillations of salinity and to periodic slow-flowing water currents. This suggests the existence of swamps connected to marine environments under warm temperate or subtropical climatic conditions.

The **b** interval is overlain by a more calcareous interval 1.20 m thick represented by marls, limey marls, marly limestones and subordinate limestones organized into a quite complex stratal package (interval c in fig. 1; see figs. 4.2 and 5.2). The heterogeneity of the lithofacies architecture is mirrored by an equivalent heterogeneity of the fossil assemblage which reflects a schizohaline environment with rapid salinity fluctuations from hypohaline to oligohaline conditions. According to the facies associations, the **c** interval can be subdivided into four portions represented by:

- c₁. 30 cm of thinly laminated foetid grey shaly marls, marls and subordinate marly limestone with *Dreissena* and *Hydrobia* together with ostracods and very rare, evidently reworked planktonic foraminifers (*Globigerinoides obliquus*, *Globigerinoides trilobus*, *Globoquadrina altispira globosa* and *Orbulina universa* in Carboni et al., 1992);

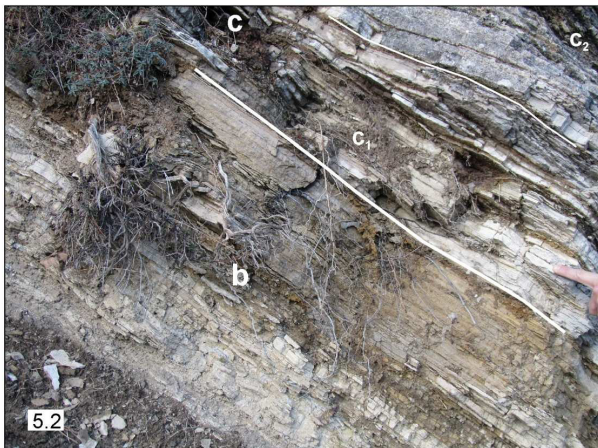
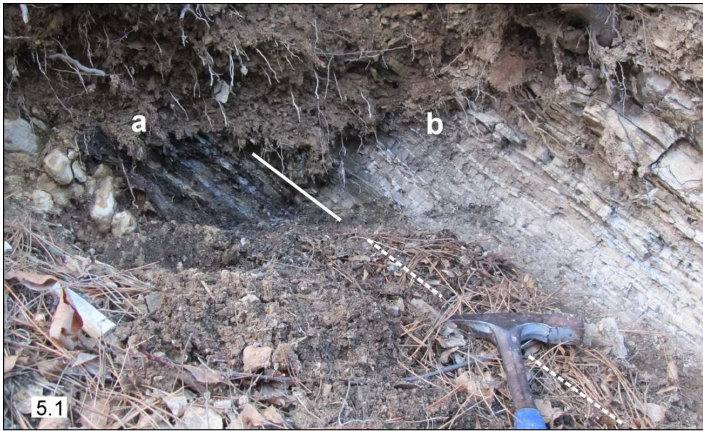


Figure 5.1. Capo di Fiume stratigraphic section. Particular of figure 4.2 showing the uppermost portion of the freshwater marsh deposits (**a**) containing a tidal-creek pebble conglomerate and the lower portion of the overlying swamp deposits (**b**) represented by laminated foetid marls. Note the gradual transition from the lower to the upper lithofacies. **5.2.** Capo di Fiume stratigraphic section. Gradual transition from the laminated swamp deposits (**b**) to the overlying brackish-water estuarine-bay deposits (**c**). **c₁** and **c₂** intervals are characterized by mollusk assemblages indicating an overall upward increase in the salinity, in concomitance with the upward increase in carbonate content.

c2. 30 cm of marls and limey marls with thin intercalations of marly limestones. The fossil assemblage, mainly represented by *Dreissena*, *Melanopsis* and small neritids belonging to the genus *Theodoxus*, together with abundant cerithiids, indicates a brackish-water environment with an overall increased salinity with respect to the underlying deposits. The microfacies (Figs. 7.1 to 7.4) is dominated by very abundant calcareous calcisphaerulids representing sporomorphs or resting cysts of algae, disarticulated valves of ostracods and thick-walled *Ammonia* associated with sporadic reworked planktonic foraminifers;

c3. 20 cm of grey marl and silty marls with thin beds of marly limestone intercalated in the lower portion and thin layers of black shales rich in organic matter and plant remains intercalated in the upper portion. The fossil assemblage is dominated by rich assemblages of potamidids and cerithioids of the families Cerithiidae, Diastomidae and Litiopidae, alternated with nearly monospecific associations of *Dreissena* concentrated in thin lumachella layers (Fig. 8.1). The occurrence of anoxic black horizons, the potamidid-cerithioid-*Dreissena* assemblages suggest a further increase in salinity with respect to the underlying deposits; the presence of hygrophilous terrestrial gastropods (vertiginids), even though very rare, may be related to episodic lowering of the salinity;

c4. 40 cm of limey marls and marly limestones with a limestone bed at the top. The fossil association characterizing this interval is dominated by *Dreissena*, *Melanopsis*, *Theodoxus*, cerithiids and small marine bivalves apparently belonging to the semelids associated with rare specimens of *Corbula*. The microfacies of the c4 portion is characterised by a groundmass

of calcareous sporomorphs with dispersed disarticulated valves of ostracods and very rare displaced planktonic foraminifers. The appearance of the first marine mollusks indicates a brackish-water environment in proximity of an open-marine shelf possibly represented by an estuarine bay.

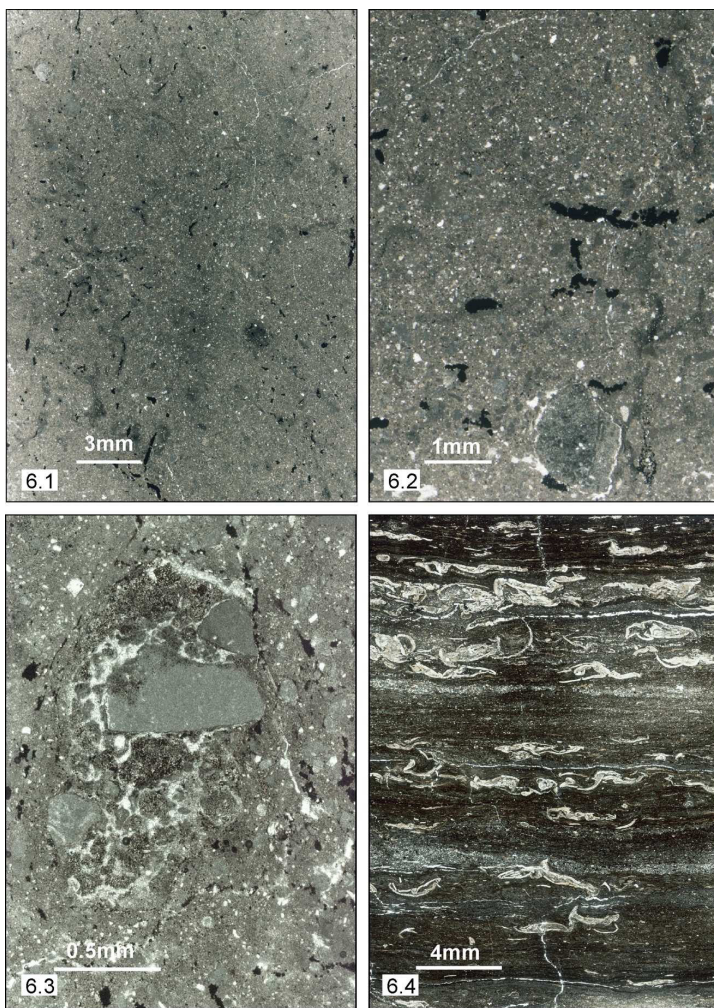


Figure 6.1. *Capo di Fiume stratigraphic section. Microfacies of the Messinian freshwater marsh deposits of the interval a. Grey to brownish speckled sandy micrite with dark-stained root tubules. 6.2. Capo di Fiume stratigraphic section. Microfacies of the Messinian freshwater marsh deposits of the interval a. Enlarged view of the sandy micrite showing well-preserved root tubules, some of which filled with a microaggregate of black pyrite framboids. The picture also shows an evident circumgranular crack around a nodule of carbonate rhizolith (lower side of the picture), as well as spar-filled fissures generated by syneresis processes. 6.3. Capo di Fiume stratigraphic section. Microfacies of the Messinian freshwater marsh deposits of the interval a. Pedogenically-reworked carbonate with spar-filled root cavities and syneresis features. 6.4. Capo di Fiume stratigraphic section. Microfacies of the Messinian swamp deposits of the interval b. Laminated black shales showing discontinuous thin lumachella layers with flattened gastropods and wavy to lenticular laminae of very fine calcarenite/calcsiltite with black veneers of wood fragments. Syneresis features are here represented by thin, spar-filled, transversal sinuous fissures and subhorizontal, flat shrinkage cracks.*

The **c** interval is overlain by approximately 30 metres of marine deposits (Tripoli Formation equivalent) represented by at least six cycles of alternating dark-grey calcareous marls and finely laminated diatomitic marls. The first marine cycle exhibits a relatively complex architecture whereas the overlying cycles primarily consist of sharp alternations of calcareous marls and diatomitic marls. In general, the sequence is characterised by a progressive decrease of thickness of the diatomitic marl intervals, which range from about 180 cm in the first cycle to 50 cm in the sixth one (Fig. 1). The sequence starts (base of the interval **d**₁ in Fig. 4.1) with a moderately thin (10 cm) laminated fissile calcareous marl containing very rare dreissenids and abundant *Corbula* followed by 40 cm of massive grey limey marls. The grey marls are heavily bioturbated and characterised by a relatively abundant bivalve content (primarily *Corbula gibba* with joined valves, but also oysters, cardiids, semelids and tellinids, see Fig. 8.2).

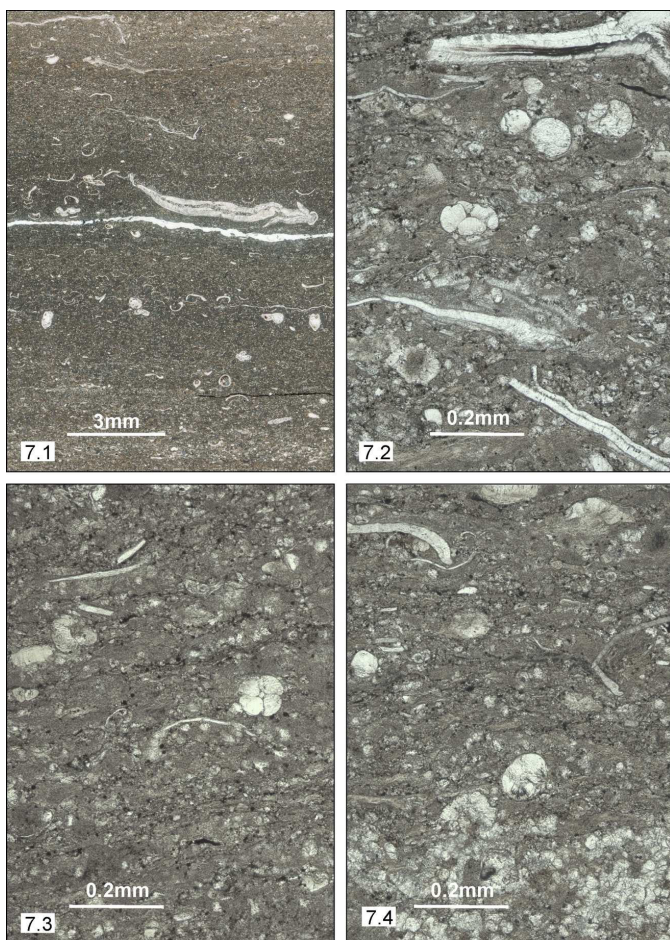


Figure 7.1. Capo di Fiume stratigraphic section. Microfacies of the Messinian estuarine-bay deposits of the interval *c*. Calcisphaerulid-rich packstone/wackestone with sparse flattened and crashed gastropods, thin-shelled bivalves and disarticulated thick-walled ostracods. **7.2** to **7.4**. Enlarged view of the calcisphaerulids. These problematic calcareous bodies, interpreted as calcitized sporomorphs or resting cysts of algae, are made up of welded microspheres of radially-arranged fibrous calcite lined by darker

sutures. In the upper left side of fig. 7.3 the broken wall in one of these spherical calcite bodies likely represents an excystation stage.

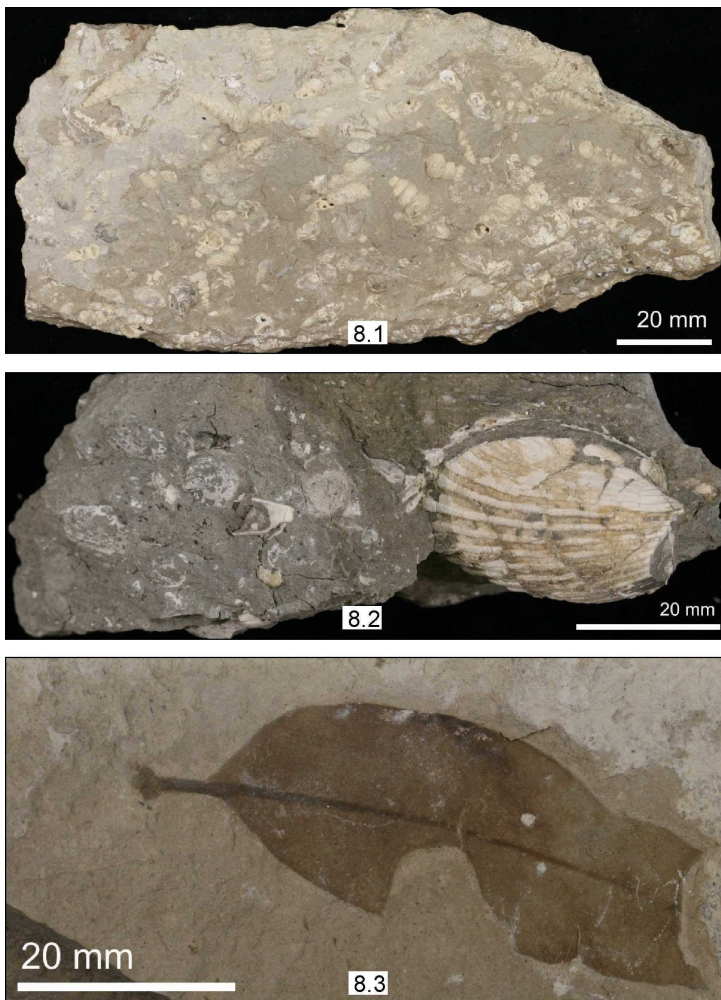


Figure 8.1. Capo di Fiume stratigraphic section. Messinian estuarine-bay deposits of the interval c_3 . Lumachella layer containing *Dreissena*, potamidids, cerithiids, litiopids, and diastomids. 8.2. Accumulation of

Corbula gibba and *Lima* sp. with conjoined valves from the grey marls at the base of the diatomitic interval d_1 of figure 4.1. 8.3. Leave from the d_1 diatomite horizon.

Carboni et al. (1992) have reported the presence of several taxa of benthic foraminifers (e.g., *Ammonia beccarii*, *Bolivina* sp., *Bulimina echinata*, *Cibicides* spp., *Elphidium crispum*) plus rare globigerinids. A centimetre-thick level of dark-brown clayey marls with mollusks separates the basal laminated calcareous marl from the overlying grey marls. The fossil assemblage of these muddy deposits indicates a marine environment characterised by very turbid waters with a maximum depth of some tens of metres (10-40 metres). The textural homogeneity and the total absence of sedimentary structures related to selective transport by marine currents or coastal drift indicate subtidal conditions in a mud-dominated open coastal flat with scarce or null sand-sized sediment supply from the catchment area. These nearshore to inner-offshore deposits are followed with abrupt contact by 180 cm of thinly laminated diatomitic marls indicative of deeper-water environment (d_1 in Figs. 1 and 4.1). The basal portion of the laminated calcareous marls is characterised by reduced diatom content, abundant plant remains (Fig. 8.3) and a moderately diverse assemblage of planktonic foraminifers (*Globorotalia* spp., *Gobigerinoides trilobus*, *Orbulina universa*). As a whole, the diatomitic marls are represented by a dense series of clastic-biogenic couplets made up of siliceous laminar mats composed of intertwined, felted diatom frustules alternating with calcisiltite laminae containing bioclastic ash, abundant siliceous sponge spicules, fish remains, scarce planktonic foraminifers, very rare fine-sand-sized quartz grains and dispersed phosphatic material trapped in a film of loose diatoms (Figs. 9.1, 9.2, 10.1 and 10.2).

The macrofossil content of this diatomitic interval is relatively rich and includes well-preserved articulated skeletal remains of not less than 22 taxa of teleost fishes belonging to 14 families, among which

the clupeid *Spratelloides gracilis* is by far the dominant element, a single nearly complete articulated skeleton assigned by Mazza et al. (1995) to the ochotonid species *Prolagus cf. apricenicus*, bird feathers, rare decapods crustaceans, insects, bivalves apparently in life position and plant remains (leaves, seeds, pine cones, fruits).

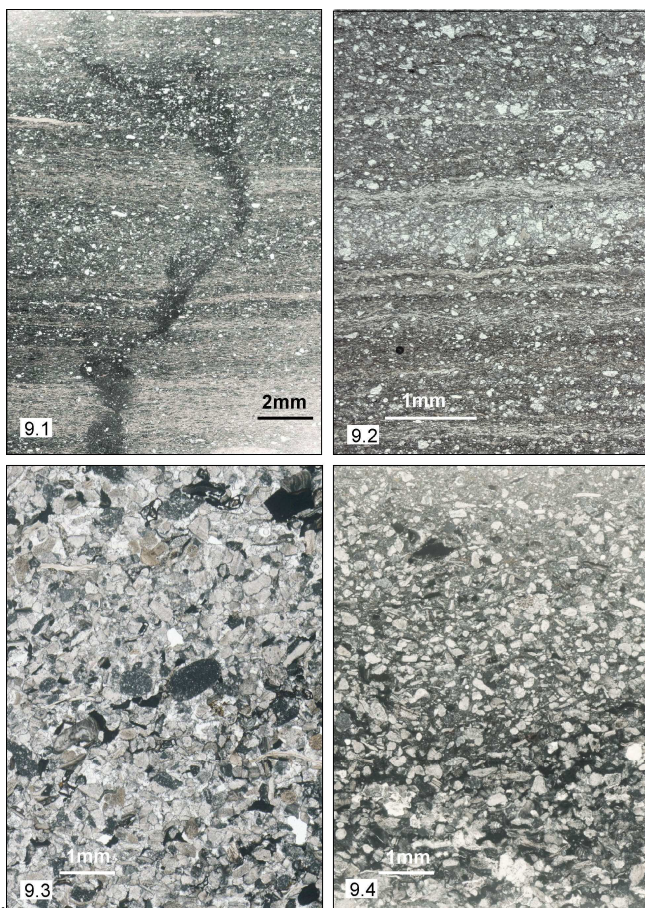
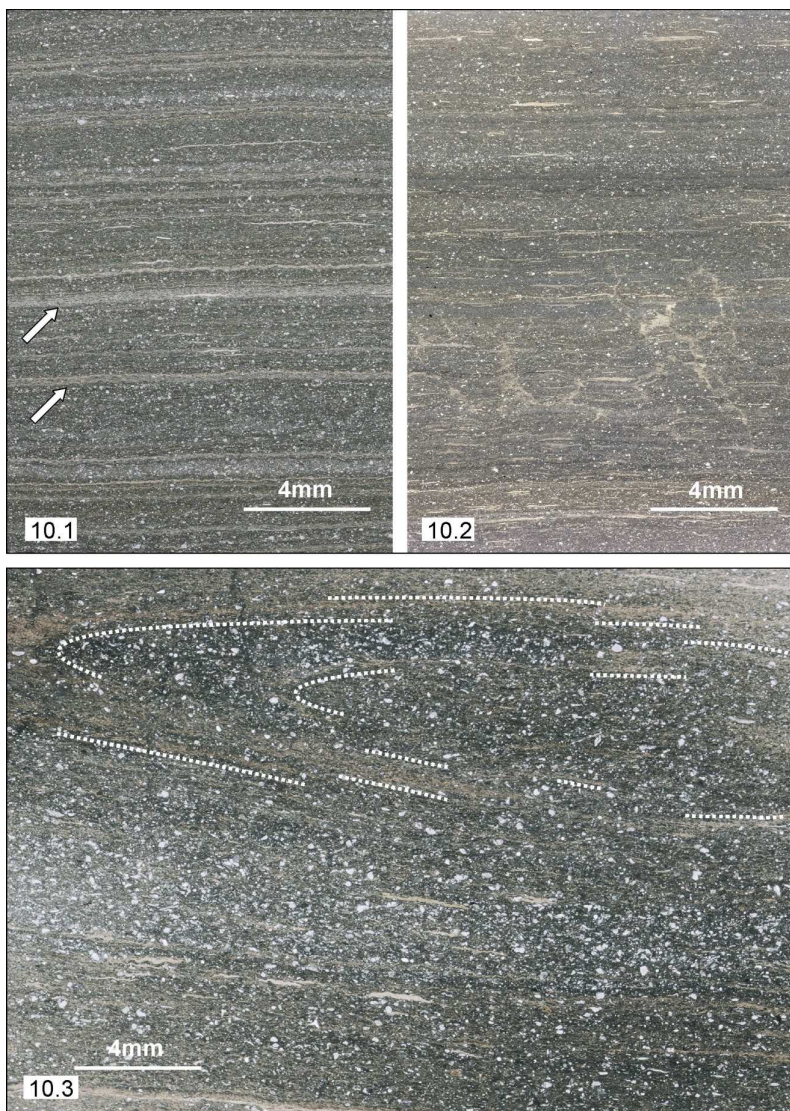


Figure 9.1. Capo di Fiume stratigraphic section. Microfacies of the Messinian deposits equivalent to the Tripoli Formation. Diatomitic marl of

the d_1 horizon. Close-up view of a dewatering microstructure preserved as a vertical pipe. Note in the lower part of the image the distinct breaking of the light-yellow diatom-rich laminae. **9.2.** Capo di Fiume stratigraphic section. Microfacies of the Messinian deposits equivalent to the Tripoli Formation. Diatomitic marl of the d_1 horizon. Enlarged view of the alternating calcisiltite and diatom-rich laminae. The coarser detrital layer in the central part of the picture is indicative of sporadic feeble traction-current processes in deep water. **9.3.** Capo di Fiume stratigraphic section. Microfacies of the Messinian deposits equivalent to the Tripoli Formation. Calciturbidite layer in the upper portion of the d_1 diatomite horizon. Bio-lithoclastic packstone with very well-rounded lithoclasts. **9.4.** Capo di Fiume stratigraphic section. Microfacies of the Messinian deposits equivalent to the Tripoli Formation. Calciturbidite layer in the Corbula-rich marls overlying the d_1 diatomite horizon. Bio-lithoclastic calcarenite with well-developed normal grading.

The rather scarce foraminifers are exclusively represented by ammoniids, bolivinids and rare dwarfed globigerinids (Carboni et al. 1992; Patacca et al. 1992). At about 20 cm from the base of the described diatomitic interval, a thin bed (7 cm thick) of massive mudstone containing a nearly monotypic assemblage of *Corbula gibba* with disarticulated and joined valves (see Fig. 8.2) has been interpreted as a subaqueous gravity-driven mud-flow deposit triggered by seismicity or by a sudden increase in the sediment loading related to a rapid sediment supply from the catchment area determined by an exceptional climatic event. Fluid-escape microstructures (Figs. 9.1. and 10.2) and microslumps (Figs. 10.3, 11.1 and 11.2) determined by seismicity or sediment loading are quite frequent in the upper portion of the diatomitic interval. These sediment-instability features are associated with centimetric calciturbidite layers commonly outlined by diagenetic black siliceous rims and affected by small-scale slumping (Fig. 11.1). The calciturbidite layers consist of coarse to medium-sand-sized recrystallized bio-lithoclastic packstones containing fragments of crustaceans, serpulids, barnacles, echinoid spines, *Elphidium* sp., fish

teeth and scales, as well as abundant, well-rounded lithoclasts derived from upper Cretaceous basinal limestones (Figs. 9.3 and 9.4).



Figures 10.1 and 10.2. *Capo di Fiume* stratigraphic section. Microfacies of the Messinian deposits equivalent to the Tripoli Formation. Diatomitic marl

of the d_1 horizon with closely spaced even-parallel laminae constituted of calcisiltites alternating with diatom-rich layers. Arrows point to some thicker light-yellow laminae made up of felted diatom frustules. In figure 10.2 an interconnected system of fluid-escape microstructures disrupts the laminae creating a kind of dish and pillar microstructures. **10.3.** Capo di Fiume stratigraphic section. Microfacies of the Messinian deposits equivalent to the Tripoli Formation. Upper portion of the d_1 horizon. Detail of a slump-related syndepositional deformation involving both calcisiltite and diatomite layers (the latter yellowish in the picture).

Several types of biogenic laminae can be recognized based on chromatic characters, thickness, lateral extension and diatom content. The diatom content is highly variable in these laminae. Laminae characterized by high clastic content often contain a moderately diverse diatom flora (*Actinocyclus* cf. *octonarius*, *Actinoptychus* sp., *Coscinodiscus* spp., *Navicula* sp., *Rhabdonema adriaticum*, *Rhaphoneis* sp., whereas other biosiliceous laminae are characterized by monospecific or oligospecific assemblages of *Coscinodiscus* spp. and/or *Thalassionema nitzschioides* (Fig. 12). The structure and composition of the *Coscinodiscus* laminae are consistent with the so-called “fall dump”, a massive sedimentation of diatoms that have grown episodically in the Deep Chlorophyll Maximum during periods of water stratification (Kemp et al., 2000), while the origin of the *Thalassionema nitzschioides* laminae is commonly associated to high productivity, nutrient abundance and bloom events (e.g., Schuette & Schrader, 1981; Sancetta, 1992). Articulated fish skeletons are primarily associated with biogenic laminae dominated by *Thalassionema nitzschioides* and/or *Coscinodiscus* sp. The excellent preservation of the skeletal remains seems to be related to the rapid mineralization mediated by microbial film that proliferated on the mucilage produced by the diatom flocs;

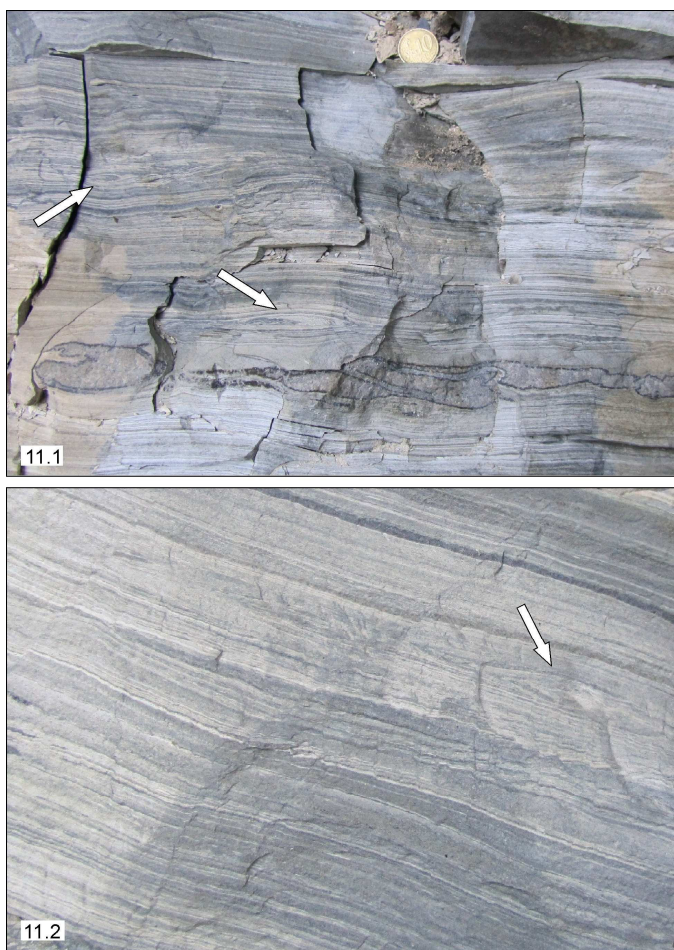


Figure 11.1. Capo di Fiume stratigraphic section. Lower portion of the Messinian deposits equivalent to the Tripoli Formation. Diatomitic horizon d_1 showing (see arrows) small-scale soft sediment deformation induced by slump mechanisms. In the lower part of the picture, a thicker slumped bed is evidenced by a diagenetic black siliceous rim. **11.2.** Capo di Fiume stratigraphic section. Lower portion of the Messinian deposits equivalent to the Tripoli Formation. Enlarged view of the diatomitic marls of the d_1

horizon showing small-scale synsedimentary deformation by slump (arrow), as well as younger brittle deformation by microfaulting.

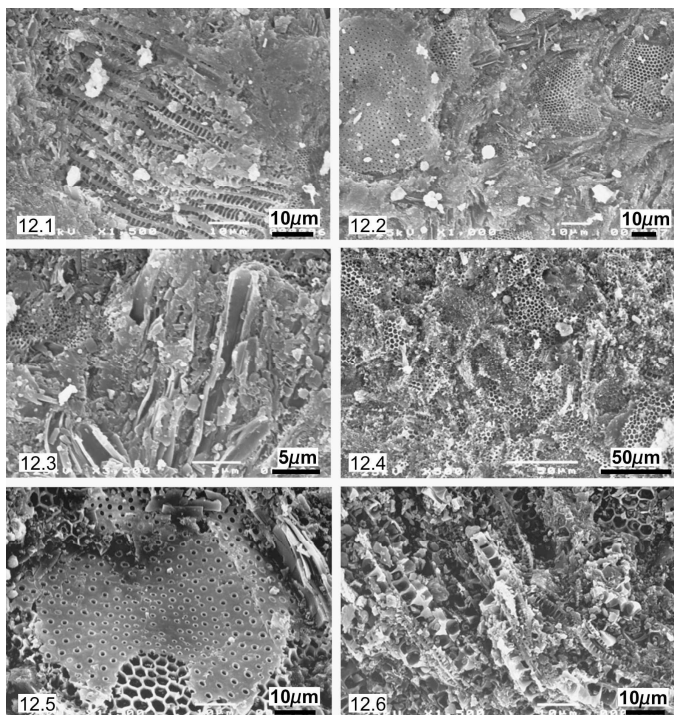


Figure 12. Capo di Fiume stratigraphic section. Scanning electron images of diatoms from the d_1 horizon. **12.1.** *Rhabdonema adriaticum*; **12.2.** *Coscinodiscus*–*Thalassionema* lamina; **12.3.** frustules of *Thalassionema nitzschioides*; **12.4.** *Coscinodiscus* lamina; **12.5.** frustule of *Coscinodiscus* sp.; **12.6.** *Coscinodiscus* lamina.

the sedimentary action of the microbial film is manifold since it protected the sediment from erosion enhancing the formation of laminated deposits, inhibited the complete decomposition of the carcasses, scavenging and endofaunal settling, and promoted the

rapid phosphatization of the bones and the mineralization of organic components.

The large part of the fossil fishes are very well preserved and nearly complete (Fig. 13). A few specimens exhibit various degrees of incompleteness, showing evidences of scavenging activity of weak hydrodynamic transport. The only recognized specimen belonging to the Nile perch, *Lates cf. niloticus*, exhibits the typical anatomical and biostratigraphical characters of a prolonged post-mortem floating. Not less than 22 taxa belonging to 14 families have been identified. The clupeid *Spratelloides gracilis* is by far the dominant element of the assemblage, represented by more than 75% of the recognized specimens. The analysis of the ecological guilds indicates that assemblage primarily consists of demersal neritic and coastal epipelagic taxa, with a subordinate contingent of migratory pelagic and oceanic species. The Nile perch is the only freshwater/paralic taxon recognized in the assemblage. The heterogeneous composition of the fish assemblage, characterized by the co-occurrence of coastal and opportunistic pelagic taxa, suggests the existence of rocky reefs and seagrass beds in close proximity to the depositional environment, and the presence of the Nile perch clearly indicates that a riversystem also contributed to the paleophysiography of the basin.

Overall, the diatom content of the biogenic laminae indicates a depositional marine environment with a water depth up to about one hundred metres. The sudden facies change from estuarine-bay to deeper-marine conditions moving from the **c** interval to the **d₁** diatomite horizon suggests a rather narrow shelf connecting coastal and basinal areas and thus favouring the accumulation of large volumes of gravity-driven deposits at a short distance from the coast.

The **d₁** diatomitic interval is overlain by about 1 metre of grey marls with intercalated centimetric calciturbidite layers (Fig.

14.1) showing evident normal grading (Fig. 9.4) and locally well-preserved erosional structures at the base. The marls contain nearly monotypic accumulations of conjoined *Corbula gibba*. The shells are

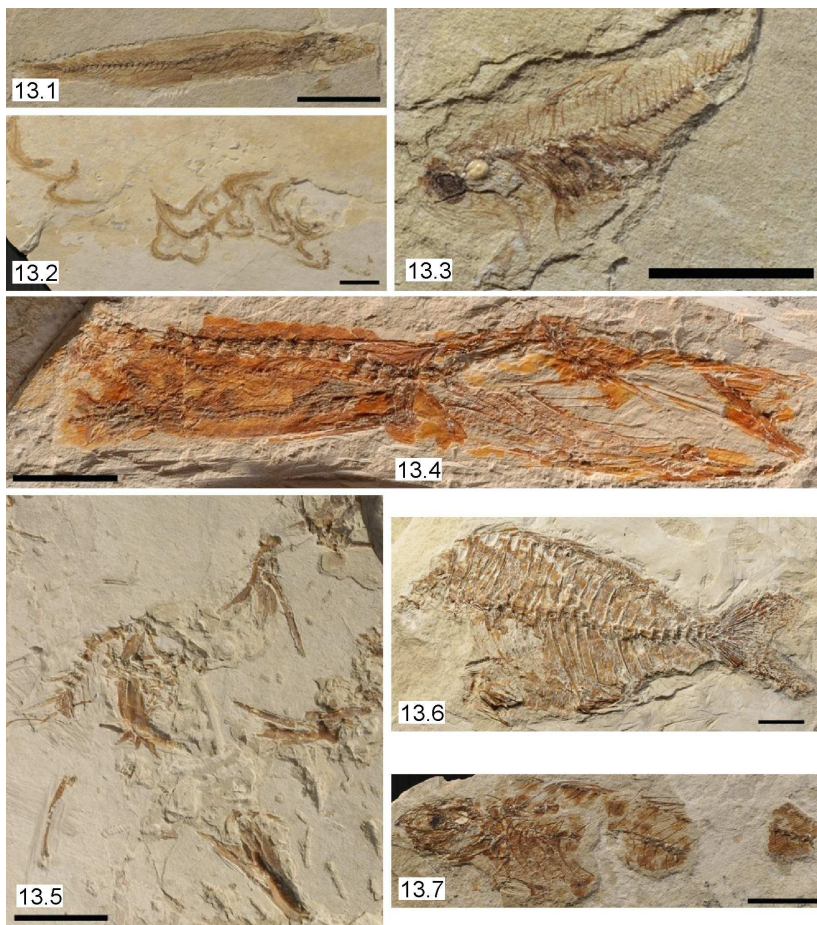


Figure 13. Capo di Fiume stratigraphic section. Fishes from the *d*₁ diatomitic horizon. **13.1.** *Spratelloides gracilis*; **13.2.** mass mortality of juvenile individuals of *Spratelloides gracilis*; **13.3.** *Diaphus edwardsi*; **13.4.** anterior portion of the body of *Paralepis albyi* with swallowed prey

specimens of Spratelloides gracilis; 13.5. *Lates cf. niloticus*; 13.6. *Pagrus sp.*; 13.7. *Boops roulei*. Scale bars 20 mm.

evidently displaced from their original position, showing the commissure parallel or sub-parallel to the bedding surfaces. The marls with calciturbidite intercalations are followed by 5 metres of massive grey marls and limey marls (Fig. 4.1) containing abundant and diversified marine bivalves (*Acanthocardia sp.*, *Callista sp.*, *Cardita sp.*, *Cardiidae indet.*, *Circomphalus sp.*, *Glans sp.*, *Lima sp.*, cf. *Megaxinus sp.*, *Ostrea sp.*, *Paphia sp.*, *Pinna sp.*, *Venus sp.*), often with joined valves, associated with rare gastropods (*Aporrhais sp.*, *Turritella sp.*). The massive aspect of this thick muddy interval, the absence of any internal sedimentary structure, the absence of biogenic reworking and the big volume of sediment involved suggest a gravitational mass-flow mechanism for transport and accumulation, perhaps triggered by seismic activity. The microfacies is characterised by very fine-grained bioclastic wackestones/packstones with dispersed and randomly distributed large mollusk fragments (Fig. 15.1) and rare small-sized *Elphidium*. The fine fraction is composed of buliminids, *Cibicides*, planktonic foraminifers (*Globigerina*, *Globogerinoides*, *Globorotalia* and *Orbulina*), abundant very thin siliceous sponge spicules, echinoid spines, unidentified bioclastic ash, abundant phosphatic material and organic particles mixed with very fine sand-to-silt-sized calcareous lithic grains (Fig. 15.2).

About 1.20 metres of finely laminated diatomitic marls lie over the massive grey limey marls. This diatomitic interval, as the previously described one, exhibits different types of indicators of tectonic instability and also contains calciturbidite beds here associated with thicker contourite-like deposits. The microfacies is similar to that of the d1 horizon, with abundant and well preserved thin sponge spicules (Figs. 15.3 and 15.4). The macrofossil content includes articulated fish skeletons, rare bivalves (*Cardita sp.*) and

plant remains, the latter extremely abundant in some biogenic laminae. Trace fossils, generally lying parallel to the bedding, are also present.



Figure 14.1. Capo di Fiume stratigraphic section. Lower portion of the Messinian deposits equivalent to the Tripoli Formation. Lower diatomitic horizon (d_1) overlain by *Corbula* marls with intercalated thin calciturbidite layers. **14.2.** Capo di Fiume stratigraphic section. Middle and upper portion of the Messinian deposits equivalent to the Tripoli Formation. d_2 - d_6 refer to diatomitic horizons the position of which is indicated in figure 1. The

diatomite horizons are separated by mud-flow deposits each bed measuring some metres in thickness.

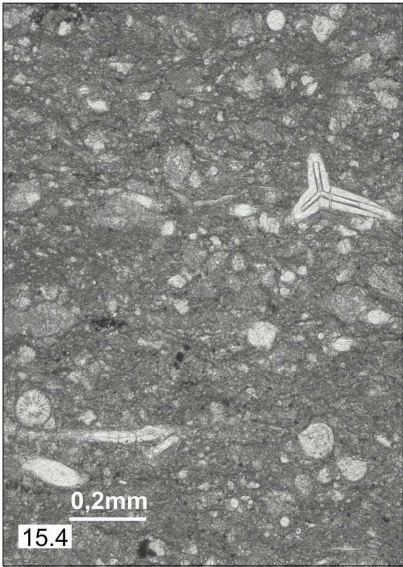
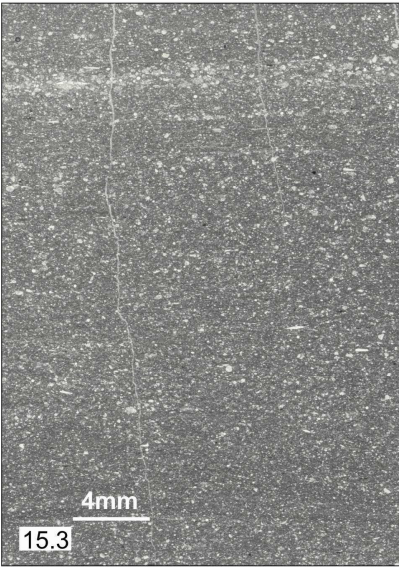
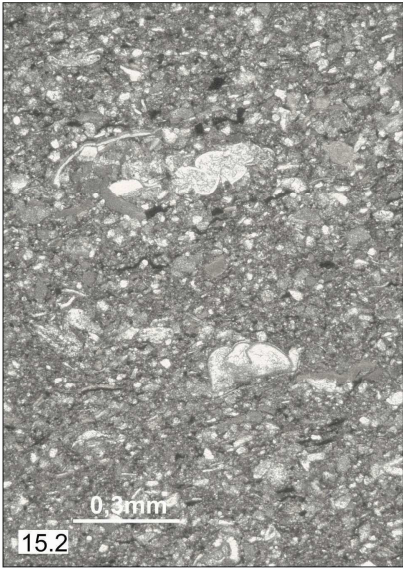


Figure 15.1. Capo di Fiume stratigraphic section. Messinian deposits equivalent to the Tripoli Formation. Microfacies representative of the massive muddy deposits overlying the d_1 diatomite horizon showing randomly distributed thin-shelled bivalves. **15.2.** Capo di Fiume stratigraphic section. Messinian deposits equivalent to the Tripoli Formation. Massive muddy interval overlying the d_1 diatomite horizon. Bio-lithoclastic wackestone/packstone with crushed buliminids (upper part of the photo). **15.3.** Capo di Fiume stratigraphic section. Messinian deposits equivalent to the Tripoli Formation. Microfacies representative of the d_2 diatomite horizon. Vaguely laminated spicule-rich packstone. A subtle parallel lamination is evidenced by the iso-orientation of the thin spicules. **15.4.** Capo di Fiume stratigraphic section. Microfacies of the Messinian deposits equivalent to the Tripoli Formation, d_2 diatomite horizon. Magnification of the microfacies of figure 10.2 showing well-preserved calcareous sponge spicules.

The succession continues with other four cycles of alternated dark grey calcareous marls and finely laminated diatomitic marls (Fig. 14.2). Each interval of dark grey calcareous marls is characterized at its base by two or three shell beds consisting of nearly monotypic assemblages of conjoined *Corbula gibba* specimens with the commissure parallel or subparallel to the bedding plane alternating with very fine-grained calciturbidites and contourites. The upper portion of the calcareous marl intervals is always characterized by common bivalves, often with joined valves and chaotic distribution, and rare turritellid gastropods. In the uppermost cycle, the dark grey calcareous marls also include a massive accumulation of large ostreids. Planktonic foraminifers are always relatively abundant. The stratigraphic marker *Turborotalia multiloba* appears to be present in the calcareous marls of the sixth cycle.

The diatomitic marls of the upper four cycles show a progressive reduction of the biogenic content and apparently lack

the previously abundant indicators of tectonic instability. Articulated skeletal remains of fishes are rare, mostly represented by poorly preserved specimens of *Spratelloides gracilis*.

References

- BELLATALLA M., GIOVANNELLI A. & MARIOTTI G. (1992) – Catena del M. Morrone, M. Pizzalto e M. Porrara: elementi e considerazioni per una loro interpretazione. *V Simposio di Ecologia e Paleoecologia delle Comunità Bentoniche*. Libro-guida delle escursioni, 121-126.
- CARBONI M.G., CIVITELLI G., CORDA L., ESU D., MATTEUCCI R. & PALAGI I. (1992) – Evoluzione delle facies e delle comunità bentoniche dal continentale al marino nel Miocene superiore della Valle del Fiume Aventino. *V Simposio di Ecologia e Paleoecologia delle Comunità Bentoniche*. Libro-guida delle escursioni, 110-120.
- CARNEVALE G. (2003) – *Tafonomia, paleoecologia e paleobiogeografia delle ittiofaune mioceniche dell'Italia Centrale*. Ph.D Thesis, Università di Pisa, 368 pp.
- KEMP A.E.S., PIKE J., PEARCE R.B. & LANGE C.B. (2000) – The “Fall dump” – a new perspective on the role of a “shade flora” in the annual cycle of diatom production and export flux. *Deep-Sea Research II*, 47: 2129-2154.
- MAZZA P., RUSTIONI M., ARUTA G. & DI CARLO E. (1995) – A Messinian *Prolagus* from Capo di Fiume Quarry (Palena, Abruzzo, Central Italy). *Bollettino della Società Paleontologica Italiana*, 34: 55-66.
- MICCADEI E. & PAROTTO M. (1998) – Assetto geologico delle dorsali Rotella-Pizzalto-Porrara (Appennino Abruzzese orientale). *Geologica Romana*, 34: 87-113.
- PATACCA E., SCANDONE P., BELLATALLA M., PERILLI N. & SANTINI U. (1992) – La zona di giunzione tra l'arco

appenninico meridionale nell'Abruzzo e nel Molise. *Studi Geologici Camerti*, volume speciale 1991/2: 417-441.

SANCETTA C. (1982) - Distribution of diatom species in surface sediments of the Bering and Okhotsk seas. *Micropaleontology*, 28: 221-257.

SCHUETTE G. & SCHRADER H. (1981) - Diatom taphocoenoses in the coastal upwelling of South West Africa. *Marine Micropaleontology*, 6: 131-155.

The *Lithothamnium* Limestone, characterized by a rich rhodalgial association, constitutes a deepening-upward sequence, conformably overlain by hemipelagic deposits (*Turborotalia multiloba* Marl), which occupies the upper portion of the Bolognano Group. The latter, usually quoted in the geological literature as the Bolognano Formation (e.g. Crescenti et al., 1969; Centamore et al., 2003) or Calcari a Briozoi e Litotamni Formation (e.g. Brandano & Corda, 2002; Pomar et al., 2004), is actually a higher-rank lithostratigraphic unit composed, in the most complete sections, of six formations (see foldout 3 in the guidebook):

- The *Lepidocyclus* Limestone and the overlying Cerratina Cherty Limestone;
- The Bryozoan Limestone and the overlying *Orbulina* Limestone;
- The *Lithothamnium* Limestone and the overlying *T. multiloba* Marl.

The Bolognano Group as a whole ranges in age from the late Oligocene to the late Miocene. The disconformities at the base of the *Lepidocyclus* Limestone, Bryozoan Limestone and *Lithothamnium* Limestone represent sequence boundaries controlled by global sea-level changes.

The chronostratigraphic scheme in foldout 3 shows that the most complete succession is exposed in Northern Majella where gaps separating the different sequences are relatively short. The succession becomes more and more incomplete moving towards the south; at the southern margin of Majella (Guado di Coccia) the Messinian portion of the *Lithothamnium* Limestone lies directly above

the Maastrichtian limestones of the Orfento Formation with a gap of about sixty million years. Such a wide stratigraphic hiatus is comparable with the one recorded in the Capo di Fiume section. The only differences between these two sections are represented by the “terra rossa” soil, present in the Capo di Fiume section and missing in the Guado di Coccia section, and by the facies of the *Lithothamnium* Limestone at Guado di Coccia and of the *Lithothamnium* Limestone equivalent at Capo di Fiume indicating respectively a marine environment with proliferation of red algae and corals (see Danese, 1999), and a coastal-transitional marine environment with an evolution from wetland to estuarine conditions.

The excursion has been planned in a way that participants can observe, along easily accessible sections, the progressive appearance of the different terms constituting the Bolognano Group and the concomitant decrease in the duration of the stratigraphic hiatuses separating the different depositional sequences. In the northernmost sections, where the hiatus between the *Orbulina* Limestone and the *Lithothamnium* Limestone is minimum or absent, the Tortonian-Messinian age of the *Lithothamnium* Limestone is well constrained by the first occurrence of *Neogloboquadrina acostaensis* in the upper portion of the *Orbulina* Limestone about 15 m. below the base of the *Lithothamnium* Limestone (Merola 2007 and by the first occurrence of *Bulimina echinata* near the top of the *Lithothamnium* Limestone.

Stop 1. Palena Cemetery

Along the Frentana Road near the Palena Cemetery (see fig. 1), the upper (Messinian) part of the *Lithothamnium* Limestone disconformably overlies Eocene nummulitid-bearing calcarenites referable to the Colle Remacinelli Formation (upper portion of the

Santo Spirito Group). In the same section the *Lithothamnium* limestones, just a few metres thick, grade upward into spicule-rich hemipelagic marls (*Turborotalia multiloba* Marl).



Figure 1. Palena Cemetery stratigraphic section. The Lithothamnium Limestone disconformably overlies the Eocene carbonates of the Santo Spirito Group and grade upwards to the *Turborotalia multiloba* Marl. **1.a.** General view on the section. **1.b.** Detail of the disconformity. The duration of the stratigraphic gap approximates 26 million years.

Figure 1b is a detail of the disconformity in which it is possible to see that the contact between the two formations follows the bedding planes with just a feeble evidence of erosion in spite of the very

important stratigraphic gap of the duration of approximately 26 million years.

Stop 2. Vallone di Taranta

In the Vallone di Taranta section, exposed along the Frentana Road about 5 kilometres north of the Palena Cemetery, the gap between the *Lithothamnium* Limestone and the Eocene Calcarenes of the Santo Spirito Group is partly filled by two new formations represented by the Langhian Bryozoan Limestone and the Serravallian *Orbulina* Limestone (Fig.2).



Figure 2. Vallone di Taranta stratigraphic section. The stratigraphic gap between the *Lithothamnium* Limestone and the Eocene carbonates of the Santo Spirito Formation is partly filled by a depositional sequence, lacking in the southernmost Majella area, made up of the Langhian Bryozoan Limestone and the Serravallian portion of the *Orbulina* Limestone Formation.

In addition, the column of the *Lithothamnium* Limestone is more complete as it includes a Tortonian portion that is lacking in the Palena Cemetery section. In this stop the Bryozoan Limestone is represented by 2-3 metres of cross-bedded bioclastic calcarenites strongly bioturbated and rich in glauconite grains in the upper

portion where the rock assumes a characteristic greenish colour. *Praeorbulina transitoria* and *P. glomerosa* s.l., present at the base of the unit, indicate the N8 Zone. Near the top, *Orbulina suturalis* immediately followed by *Orbulina universa* indicates the latest N9/earliest N10 Zones. The glauconitic calcarenites are conformably overlain by 6-8 metres of thin-bedded pelagic limestones and marly limestones belonging to the *Orbulina* Limestone Formation. The planktonic foraminifer assemblage ranges from the N9 Zone after the FCO of *Orbulina universa* to the N13 Zone after the FO of *Paragloborotalia partimlabiata*. The overlying *Lithothamnium* Limestone Formation, disconformably overlying *Orbulina* Limestone, is represented by a deepening-up succession about 15 metres thick made up of detrital limestones rich in *Ammonia* and *Elphidium* grading upward into massive rhodolith-rich limestones. Near the top of the formation, where beds are separated by thin marly layers, benthonic foraminifers of the *Bulimina echinata* Zone are present. Finally, the *Lithothamnium* Limestone is conformably overlain by hemipelagic marls rich in sponge spicules containing *Turborotalia multiloba* (*T. multiloba* Marl).

Stop 3. Colle di Votta quarry near Abbateggio

In this stop the Messinian evaporites of the Gessoso-Solfifera Formation are exposed in the artificial section of an abandoned quarry. The section is constituted by some metres of massive selenite overlain by a thinning-upward sequence 25-30 metres thick made up of gypsum (selenites, gypsrudites, gypsarenites, and laminated gypsum) alternating with sapropelic black shales more frequent and thicker in the upper part (Fig. 3).



Figure 3. Artificial section in the evaporites of the Messinian Gessoso-Solfifera Formation near Abbateggio.

Stop 4. Roccamorice

In the northern Majella area all lithostratigraphic units forming the Bolognano Group are present, with the three almost complete depositional sequences each of them represented by inner or shallow middle-ramp transgressive calcarenites grading upwards into outer-ramp hemipelagic carbonate deposits:

Sequence 1, represented by the *Lepidocyclina* Limestone, conformably followed by the Cerratina Cherty Limestone (Chattian-Aquitania);

Sequence 2, represented by the Bryozoan Limestone conformably followed by the *Orbulina* Limestone (Burdigalian-Tortonian p.p.);

Sequence 3 represented by the *Lithothamnium* Limestone conformably followed by the *T. multiloba* Marl (Tortonian p.p.-Messinian).

The three sequences are separated by very short gaps, as indicated in the chronostratigraphic scheme of foldout 3.

A complete section of the *Lithothamnium* Limestone Formation around 15 m thick can be observed near Roccamorice along the road connecting this village with San Valentino in Abruzzo Citeriore. The stratigraphic contact between the *Lithothamnium*

Limestone and the underlying *Orbulina* Limestone is well exposed in the wall of a gorge delimiting Roccamorice in the west (Fig. 4.1). In the same valley the middle-upper portion of the *Orbulina* Limestone are also very well exposed (Fig. 4.2). The lowest terms are constituted of a few metres of nodular calcilutites, marly calcilutites and subordinate marls appearing in thin section as planktonic-foram wackestones. This portion is characterized by a pervasive bioturbation represented by burrowing parallel to the bedding and by frequent casts of *Zoophycus*. The nodular calcilutites are followed by about 15 metres of grey calcisiltites and very fine-grained calcarenites. In this interval burrowing parallel to the bedding is still frequent, but vertical traces are also developed and become prevalent in the upper part of the interval. In thin section the calcisiltites/calcarenites appear as bioclastic packstones/wackestones rich in planktonic foraminifers, echinoid spines, subordinate benthic foraminifers and unidentified biotritus. In terms of sequence stratigraphy, the coarser-grained sediments of the second interval have been interpreted as the high-stand systems tract subsequent the maximum flooding.

Figure 5 shows a columnar section of the *Lithothamnium* Limestone in the Roccamorice area which has been correlated with a columnar section of the *Lithothamnium* Limestone cropping out at Scontrone Cemetery. The two sections are basically identical, apart from the high-energy bars at the base of the *Lithothamnium* Limestone of Scontrone Cemetery which were deposited on an inner ramp during the marine transgression and did not develop in the more distal depositional domain of the northern Majella area. The **a-e** intervals in the left side of the Scontrone Cemetery column indicate

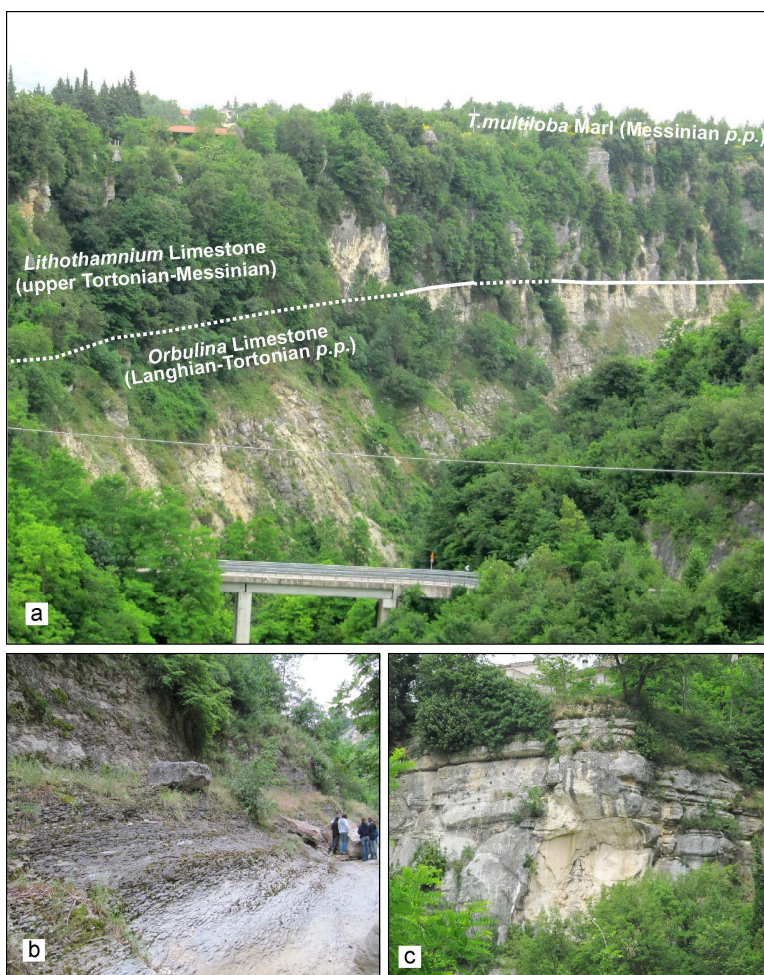


Figure 4. Roccamorice stratigraphic section in the Tortonian-Messinian Lithothamnium Limestone. **4.a.** General view of the contact between the Orbulina Limestone and the Lithothamnium Limestone formations in the gorge west of Roccamorice. **4.b.** Detail of the Orbulina Limestone in the same gorge of figure 4.a. **4.c.** Upper portion of the Lithothamnium Limestone. The Messinian benthic foraminifer *Bulimina echinata* has been found at the top of this interval.

the major deepening steps of the sedimentary sequence. Examples of microfacies characterizing the different intervals are provided in the a-e pictures. The first interval, present only in the Scontrone area, is represented by 3 metres of lithobioclastic calcarenites displaying large-scale and low-angle cross stratification. The microfacies (picture a in Fig. 5) is represented by fine to medium-grained bioclastic packstones/grainstones with large-sized *Ammonia* (lower and upper left side of the picture) and *Elphidium crispum* (upper right side). The characteristic *Ammonia*-and-*Elphidium* association and the evident winnowing of the sediment suggest a nearshore environment with reduced salinity.

Interval **b**, displaying identical characteristics both in the Scontrone and Roccamorice areas, consists of 2 metres of bioclastic calcarenites rich in *Heterostegina*, deposited on a shallow middle ramp. In thin section (picture b in Fig. 5) these calcarenites appear as coarse-grained litho-bioclastic packstones rich in abraded skeletal particles, fragmented red-algal rhodoids (lower left side of the microphotograph) and *Heterostegina* (upper right side) associated with *Elphidium crispum* (centre). The *Heterostegina*-bearing calcarenites are overlain by about 10 metres of massively-bedded limestones and subordinate marly limestones rich in *Lithothamnium thallii* that form well-developed rhodoliths (interval **c**). The depositional environment was a deeper middle ramp. Thin sections from this portion of the unit show a rhodolith floatstone with very large composite red algal-bryozoan rhodoids set in a silty bioclastic matrix (picture c in Fig. 5). The litho-biofacies of this relatively muddier interval points to a low-energy mid-ramp setting with temperate water. Interval **c** is overlain by about 3 metres of bedded marly limestones with thin marly interlayers (interval **d** in Fig. 5; see also Fig. 4.3) deposited over an outer ramp. The marly limestones still contain dispersed *Lithothamnium thallii* together with bivalves, mostly pectinids. Occasional beds of *Heterostegina*-bearing

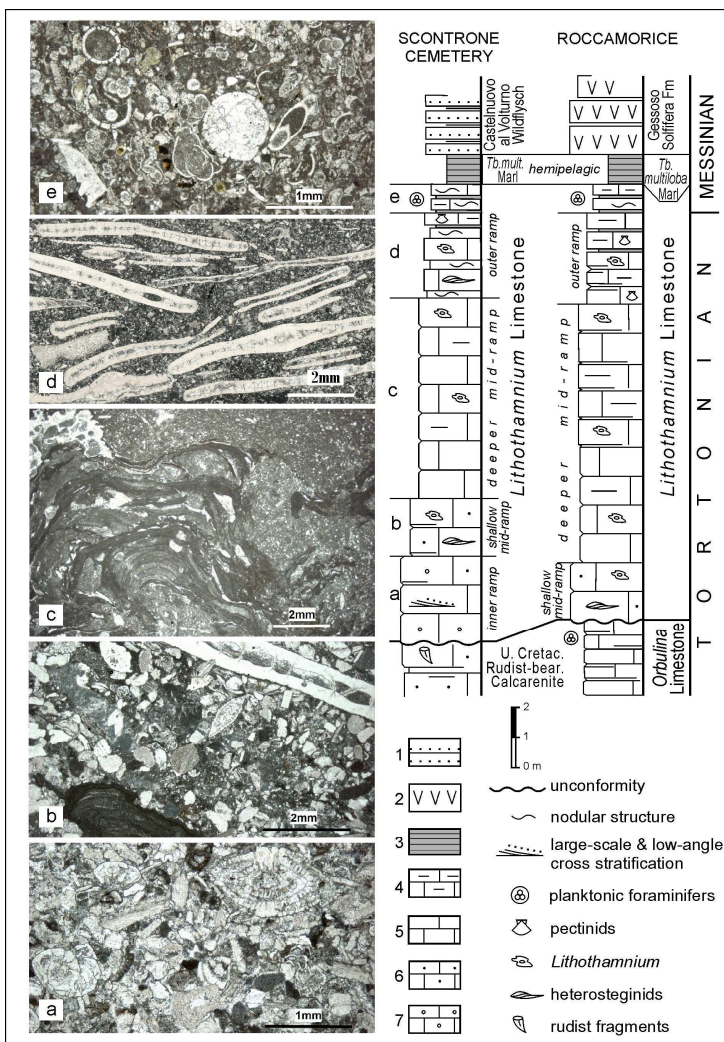


Figure 5. Columnar section of the *Lithothamnium Limestone* Formation in the Roccamorice area and correlation with the *Lithothamnium Limestone* exposed in the Scontrone Cemetery section. Explanations are in the text. 1, Fine-grained sandstones; 2, gypsum; 3, Marls and calcareous

marls; 4, Marly limestones; 5, Calcilutites; 6, Bioclastic calcarenites; 7, Bioclastic calcarenites with oversized lithoclasts.

calcarenites (packstones rich in *Heterostegina* associated with fragmented echinoid spines and scattered planktonic forams, see picture e in Fig. 5) represent sporadic storm accumulations on an open, warm/temperate outer-ramp setting below fair weather wave base. The uppermost portion of the *Lithothamnium* Limestone is everywhere represented by 1 metre of condensed marly limestones with clayey interlayers (interval e in Fig. 5). In thin section (picture e in Fig. 5) these marly limestones appear as foraminiferal packstones with large-sized *Orbulina universa* (e.g., in the centre and at the upper left side of the microphotograph), subordinate bolivinids and other benthic forams with hyaline calcareous well. The abundance of phosphatic coprolites and large, rounded glauconite grains together with the strong bioturbation suggest that these condensed marly limestones were deposited in a starved outer-ramp setting. The condensed interval has been attributed to the early Messinian because of the diffuse presence of *Rectuvigierina* characterizing the *Bulimina echinata* Zone of Colalongo & Sartoni (1979). This moment represents at the regional scale a moment of maximum flooding and of maximum landward encroachment of the shoreline in the innermost portions of the carbonate ramp which allow useful temporal correlations between shallow and deeper marine environments in the whole study area.

The *Lithothamnium* Limestone is everywhere conformably overlain by spicule-rich marls containing the marker *Turborotalia multiloba* (*T. multiloba* Marl). The first common occurrence of *Turborotalia multiloba* has been astronomically positioned at 6.415 Ma (see Hilgen & Krijgsman, 1999; Sierro et al., 2001).

In the Scontrone Cemetery section the *Lithothamnium* Limestone overlies the upper Albian-Turonian Rudist-bearing

Calcarenites with a remarkable hiatus between the two lithostratigraphic units. In the Roccamorice section, on the contrary, no significant temporal gap separates the *Lithothamnium* Limestone from the underlying *Orbulina* Limestone. Careful biostratigraphic investigations in the entire northern Majella area (Merola, 2007) allowed the recognition of important bioevents defining the age of the upper portion of the *Orbulina* Limestone: last occurrence of *Paragloborotalia siakensis* (about 15 metres below the top of the formation) immediately followed by the first occurrence of *Neogloboquadrina atlantica* and finally by the first occurrence of *Neogloboquadrina acostaensis*. The last occurrence of *Pg. siakensis* marks the top of the N14 Blow's Zone while *N. acostaensis* is a base marker of the N16 Zone (Blow 1969). The first occurrence of the *Neogloboquadrina* group falls very close to the GSSP (Global boundary Stratotype Section and Point) of the Tortonian stage recently established in the Monte dei Corvi section near Ancona (Italy) which has been astronomically dated at 11.608 Ma (Hilgen et al., 2005).

In the Scontrone area it is impossible to date the base of the *Lithothamnium* Limestone, and therefore it is impossible to date by direct evidence the vertebrate-bearing deposits. In the Roccamorice section, on the contrary, the base of the *Lithothamnium* Limestone is chronologically well constrained by the Serravallian-Tortonian boundary recognized in the uppermost portion of the *Orbulina* Limestone. The boundary between the Tortonian portion of the *Lithothamnium* Limestone and the Messinian one is not well defined, but the recognition of the *Bulimina echinata* Zone at the top of the formation indicates, in any case, that the bulk of the limestones have a Tortonian age. Consequently, the terrestrial vertebrates of Scontrone, contained in deposits that occupy a basal position in the *Lithothamnium* Limestone Formation, cannot be younger than the Tortonian.

References

- BLOW W. (1969) – Late-Middle Eocene to Recent planktonic foraminiferal biostratigraphy. In: BRONNIMAN P. & RENZ M.M. (Eds.) “Proceeding of the First International Conference on Planktonic Microfossils” (Geneve 1967). Leiden, E. J. Broll, 1: 199-421.
- BRANDANO M. & CORDA L. (2002) – Nutrients, sea level and tectonics: constraints for the facies architecture of a Miocene carbonate ramp in Central Italy. *Terra Nova*, 14: 257-262.
- CENTAMORE E., PRATURLON A. & RUSCIADELLI G. (2003) – Inquadramento geologico e lineamenti di paleogeografia, stratigrafia e paleontologia. In CRESCENTI U., MICCADEI E. & PRATURLON A. (Eds.), pp. 15-27. *Guide Geologiche Regionali – 15, Itinerari Abruzzo*. Società Geologica Italiana.
- COLALONGO M.L. & SARTONI S. (1979) – Schema biostratigrafico per il Pliocene ed il basso Pleistocene in Italia. Note Preliminari per la Carta Neotettonica d’
- CRESCENTI U., CROSTELLA A., DONZELLI G. & RAFFI G. (1969) – Stratigrafia della serie calcarea dal Lias al Miocene nella regione marchigiano-abruzzese. (Parte II. Litostratigrafia, Biostratigrafia, Paleogeografia). *Memorie della Società Geologica Italiana*, 8: 343-420.
- DANESE E. (1999) – Upper Miocene carbonate ramp deposits from the southernmost part of Maiella Mountain (Abruzzo, Central Italy). *Facies*, 41: 41-54.
- HILGEN F., ABDUL AZIZ H., BICE D., IACCARINO S., KRIJGSMAN W., KUIPER K., MONTANARI A., RAFFI I., TURCO E. & ZACHARIASSE W.-J. (2005) – The Global boundary Stratotype Section and Point (GSSP9 of the

- Tortonian Stage (Upper Miocene) at Monte dei Corvi. *Episodes*, 28: 6-17.
- HILGEN F.J. & KRIJGSMAN W. (1999) - Cyclostratigraphy and astrochronology of the Tripoli diatomite formation (pre-evaporite Messinian, Sicily, Italy). *Terra Nova*, 11: 16-22.
- MEROLA D. (2007) - Biostratigrafia a foraminiferi planctonici dei depositi emipelagici dell'Oligocene Superiore/Miocene Inferiore (Calcarei con Selce) e del Miocene Medio (Calcilutiti ad *Orbulina* della Montagna della Maiella (Appennino centrale, Abruzzo). Ph.D Thesis, Università di Pisa.
- POMAR L., BRANDANO M. & WESTPHAL H. (2004) - Environmental factors influencing skeletal grain sediment associations: a critical review of the Miocene examples from the western Mediterranean. *Sedimentology*, 51: 627-651.
- SIERRO F.J., HILGEN F.J., KRIJGSMAN W. & FLORES J.A. (2001) - The Abad composite (SE Spain): a Messinian reference section for the Mediterranean and the APTS. *Palaeogeography, Palaeoclimatology, Palaeoecology*, 168: 141-169.

